(NASA-CR-161224) THERMAL AND FLUID FLOW ANALYSES OF SOUNDING ROCKET EXPERIMENT 74-21/2R AND 74-21/3R Final Report (Lockheed Missiles and Space Co.) 73 p HC A04/MF A01 CSCL 20D G3/34

N79-24295

Unclas 20891

[redacted]

Lockheed

HUNTSVILLE RESEARCH & ENGINEERING CENTER

LOCKHEED MISSILES & SPACE COMPANY, INC.
A SUBSIDIARY OF LOCKHEED CORPORATION

HUNTSVILLE, ALABAMA

LMSC-HREC TR D568959

Lockheed

Missiles & Space Company, Inc.

HUNTSVILLE RESEARCH & ENGINEERING CENTER

Cummings Research Park
4800 Bradford Drive,
Huntsville, Alabama

THERMAL AND FLUID FLOW ANALYSES OF SOUNDING ROCKET EXPERIMENTS 74-21/2R AND 74-21/3R

FINAL REPORT

April 1979

Contract NAS8-32422

Prepared for National Aeronautics and Space Administration
Marshall Space Flight Center, Alabama 35812

by

S. J. Robertson

APPROVED: S. V. Bourgeois, Supervisor
Industrial Environmental R&E Section

J. S. Farrior
Resident Director

FOREWORD

This document reports the results of a three-month study by personnel of the Lockheed-Huntsville Research & Engineering Center, under Contract NAS8-32422 for the National Aeronautics and Space Administration, George C. Marshall Space Flight Center. The stated contract requirements are:

1. Provide analytical support for fluid flow phenomena in Sounding Rocket Experiments 74-21/2R and 74-21/3R.
2. Evaluate the extent of fluid flow and determine the thermal profiles in Experiments 74-21/2R and 74-21/3R under ground-based and actual flight conditions.

The NASA technical monitor for this contract was Dr. Mary Helen Johnston of NASA-MSFC Materials and Processes Laboratory.

CONTENTS

Section		Page
	FORWORD	ii
1	INTRODUCTION AND SUMMARY	1
2	EXPERIMENT DESCRIPTION	3
3	RESIDUAL FLOW VELOCITIES AFTER DE-SPIN	9
4	THERMAL/CONVECTION ANALYSIS	12
	4.1 Results for 74-21/2R Flight Test	12
	4.2 Results for 74-21/3R Flight Test	
	4.3 Results for 74-21/2T, Ground Test	58
	4.4 Results for 74-21/3R, Ground Test	61
5	SOLUTAL CONVECTION ANALYSIS	64
6	CONCLUSIONS	68
	REFERENCES	69

1. INTRODUCTION AND SUMMARY

The Sounding Rocket Experiments 74-21/2R and 74-21/3R were intended to study the crystalization of a 27.8 percent ammonium chloride aqueous solution under conditions of low gravity. The two experiments consisted of rectangular containers of solution with the crystalization driven by cooling one or more faces of the containers by thermo-electric cooling devices. The containers were filled completely and sealed to eliminate any significant pockets of air. Experiment 74-21/2R consisted of a 1/2 cm x 1 cm x 4 cm quartz container of solution cooled on one of the 1/2 cm x 1 cm faces. Experiment 74-21/3R consisted of a 1 cm x 1 cm x 4 cm plexiglass container cooled on one of the 1 cm x 1 cm faces and on two opposing 1 cm x 4 cm faces. The low gravity portion of the flight lasted approximately 3 1/2 minutes with g levels on the order of 10^{-5}. Temperature measurements were made at several points on the outside of the containers to enable analysis of heat transfer and the resulting convective motion in the containers. Ground tests were made with the long dimensions of the containers in the vertical position to compare with flight results.

The Lockheed-Huntsville thermal analyzer and LOCAP convective analyzer programs were used to analyze the test results. The ground test convective analyses and the solutal convective analyses were based on well known closed form convective equations, rather than the LOCAP program, because of excessively long run times required in the program at high gravity levels and high concentration gradients. Thermal convection velocities on the order of 10^{-5} cm/sec were calculated using the LOCAP program for the flight tests, compared to estimates of about 0.5 cm/sec for the ground tests. Solutal convection velocities of about 0.002 cm/sec were estimated for the flight tests compared to about 0.5 cm/sec for the ground tests. Note that

the solutal and thermal convective velocity estimates are about the same for the ground tests. The solutal effects, however, are confined to a layer about 1 mm thick near the solidifying interface.

2. EXPERIMENT DESCRIPTION

The two experiments were housed in the sounding rocket in the orientations shown in Fig. 1. The cooling devices were actuated at 60 sec into the flight for 74-21/2R and 30 sec for 74-21/3R. During the launch phase of the flight, the rocket was spin-stablized with a spin rate of about 240 rpm. At about 70 sec, the rocket under went de-spin, and at 90 sec, powered flight ended and the low gravity period begun. The low gravity portion of the flight continued until about 360 sec flight time. Photographs were taken throughout the low g portion of the flight.

Thermistor temperature measuring devices were attached to the outside of the containers at several locations to permit an analysis of heat transfer throughout the containers and the ammonium chloride solution in the containers. The temperature histories thus determined along the fluid bound aries were then used as boundary conditions for an analysis to determine convective fluid motions. Figure 2 shows the experiment configurations and the locations of the temperature measurements on both the 74-21/2R and 74-21/3R experiments.

The gravity levels during flight as measured by on-board accelerometers, are shown in Figs. 3 through 5 for the components in the vehicle X, Y, Z coordinate directions (See Fig. 1 for orientation of experiments with respect to these directions). Zero flight time was taken at 15:59:10 (hrs, min, sec) on the day of launch.

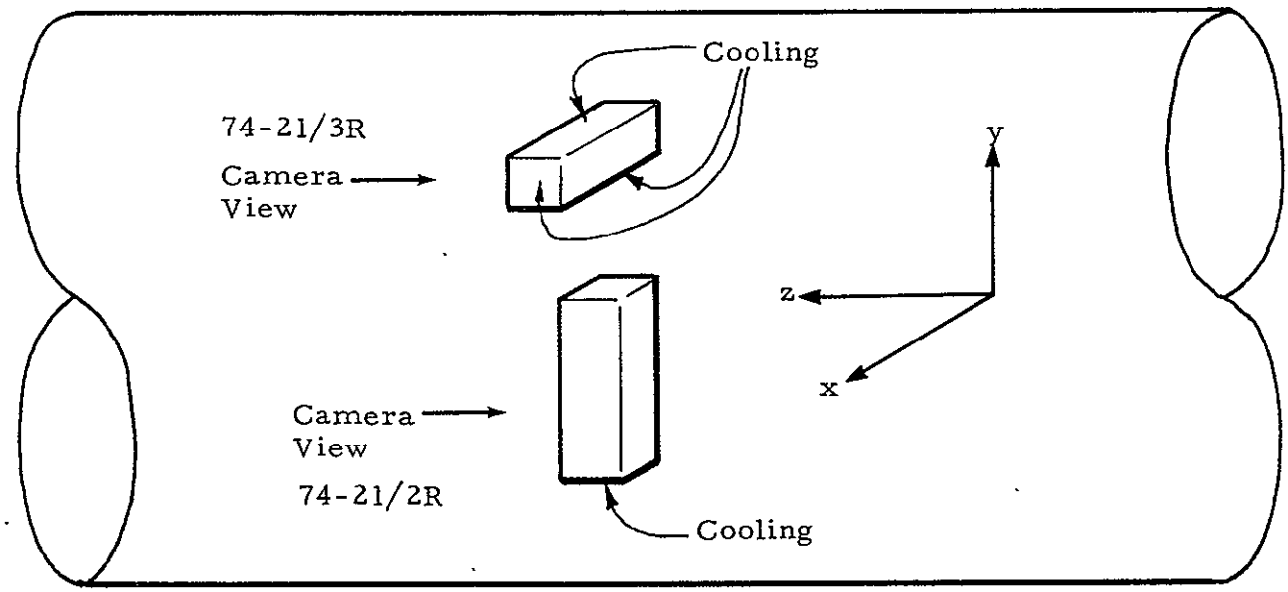

Fig. 1 - Orientation of Experiments 74-21/2R and 74-21/3R in Sounding Rocket

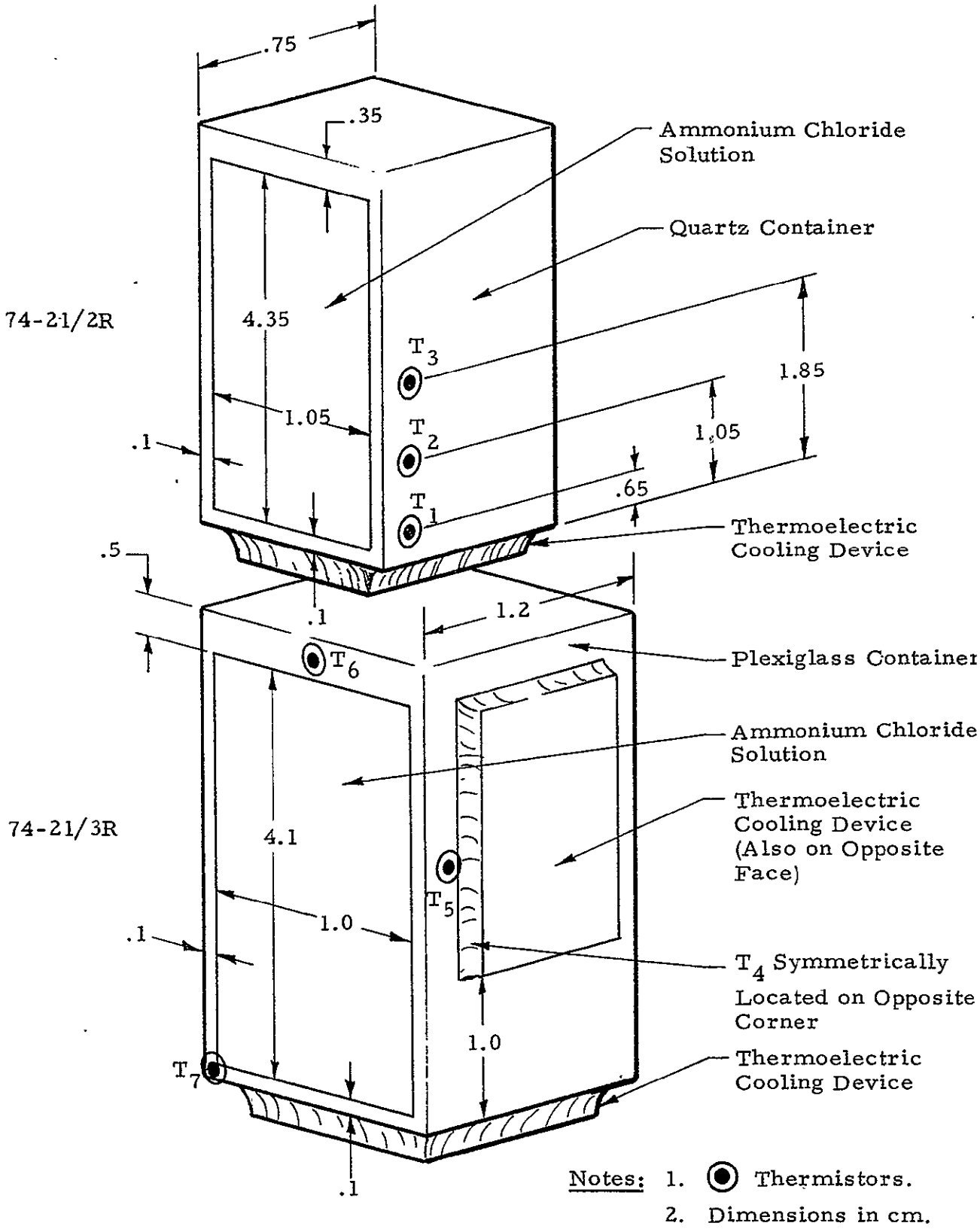

Fig. 2 - Geometry of Experiments 74-21/2R and 74-21/3R with Locations of Temperature Measurements

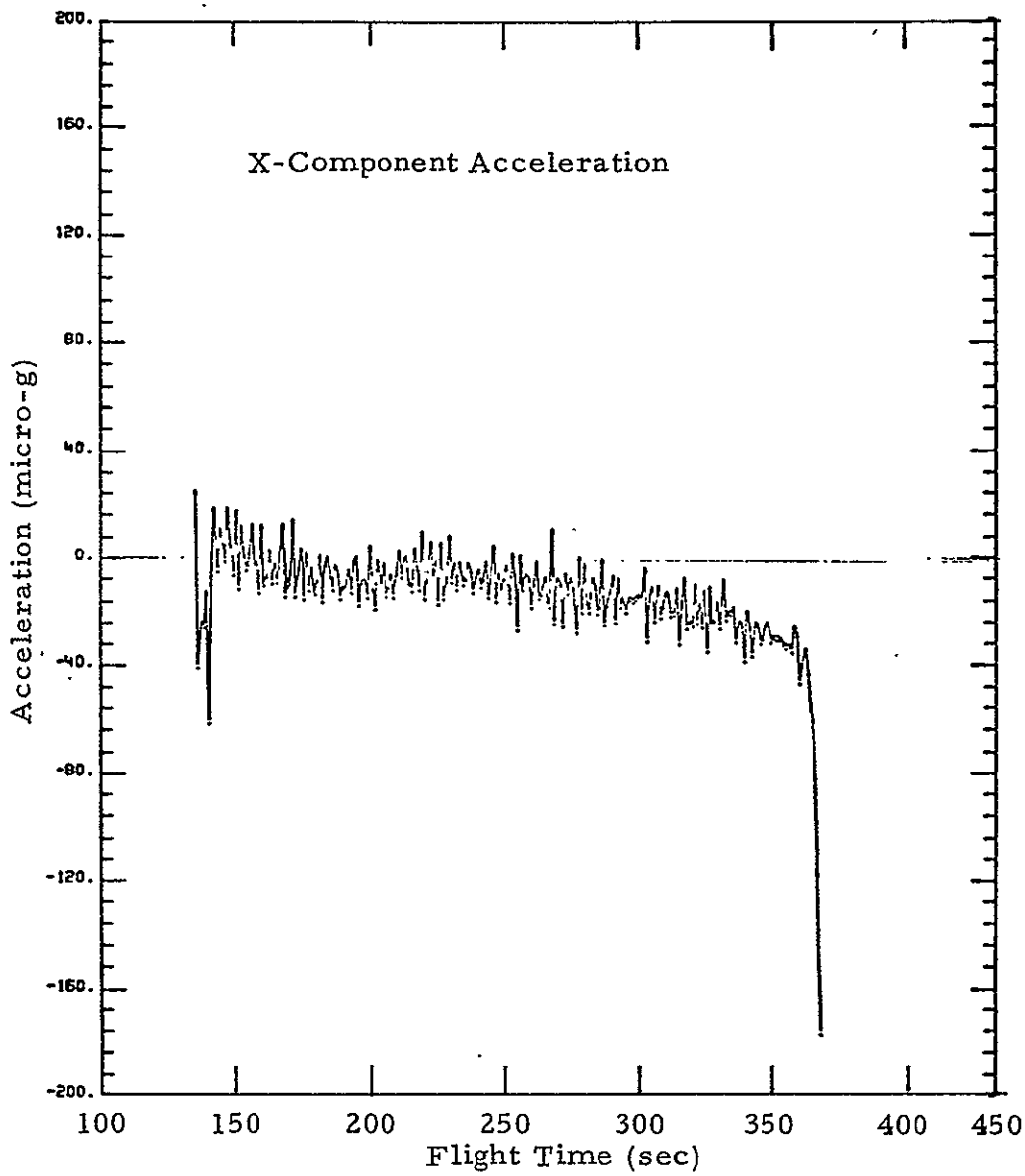

Fig. 3 - Gravity Level in X Direction During Flight

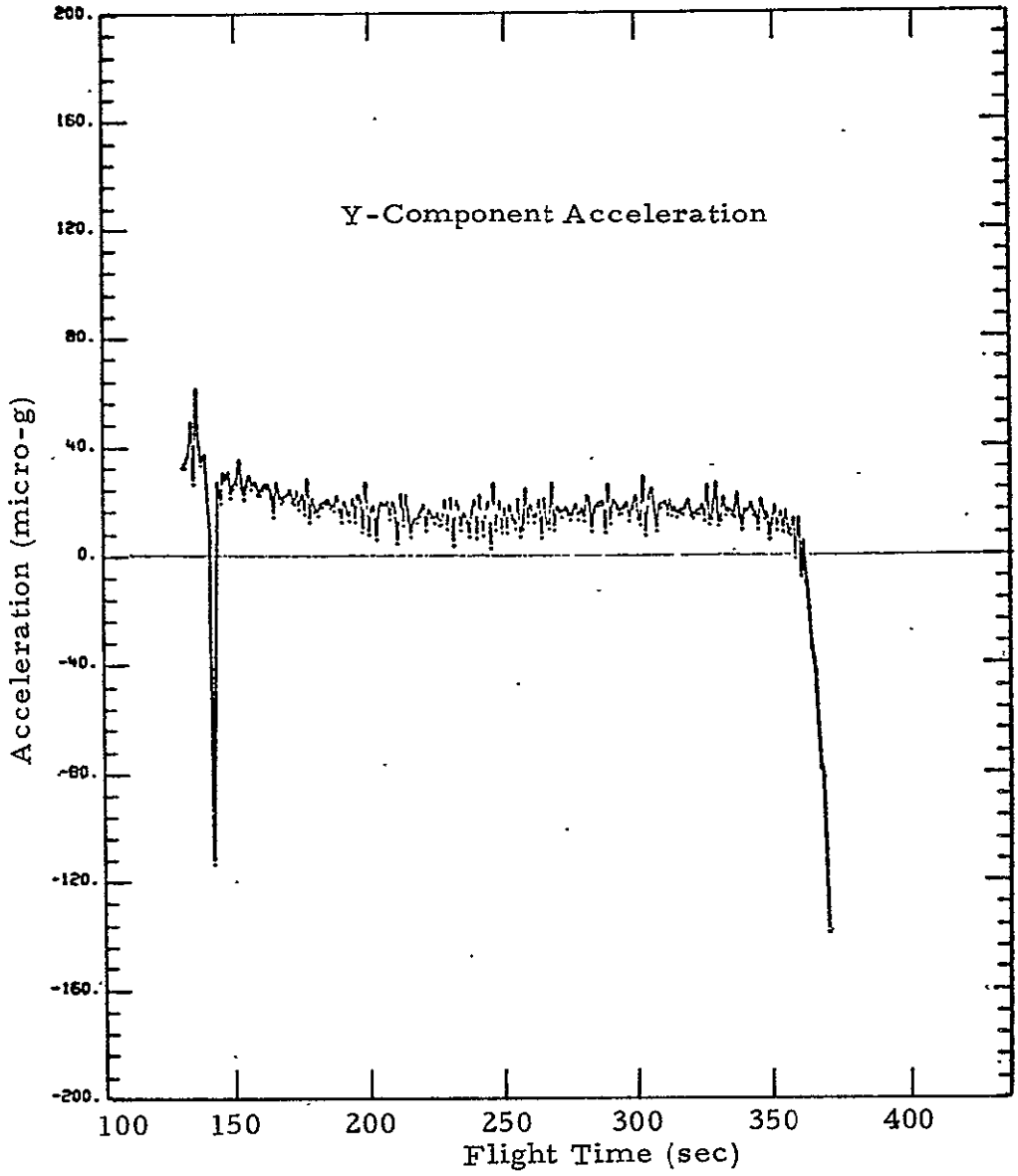

Fig. 4 - Gravity Level in Y Direction During Flight

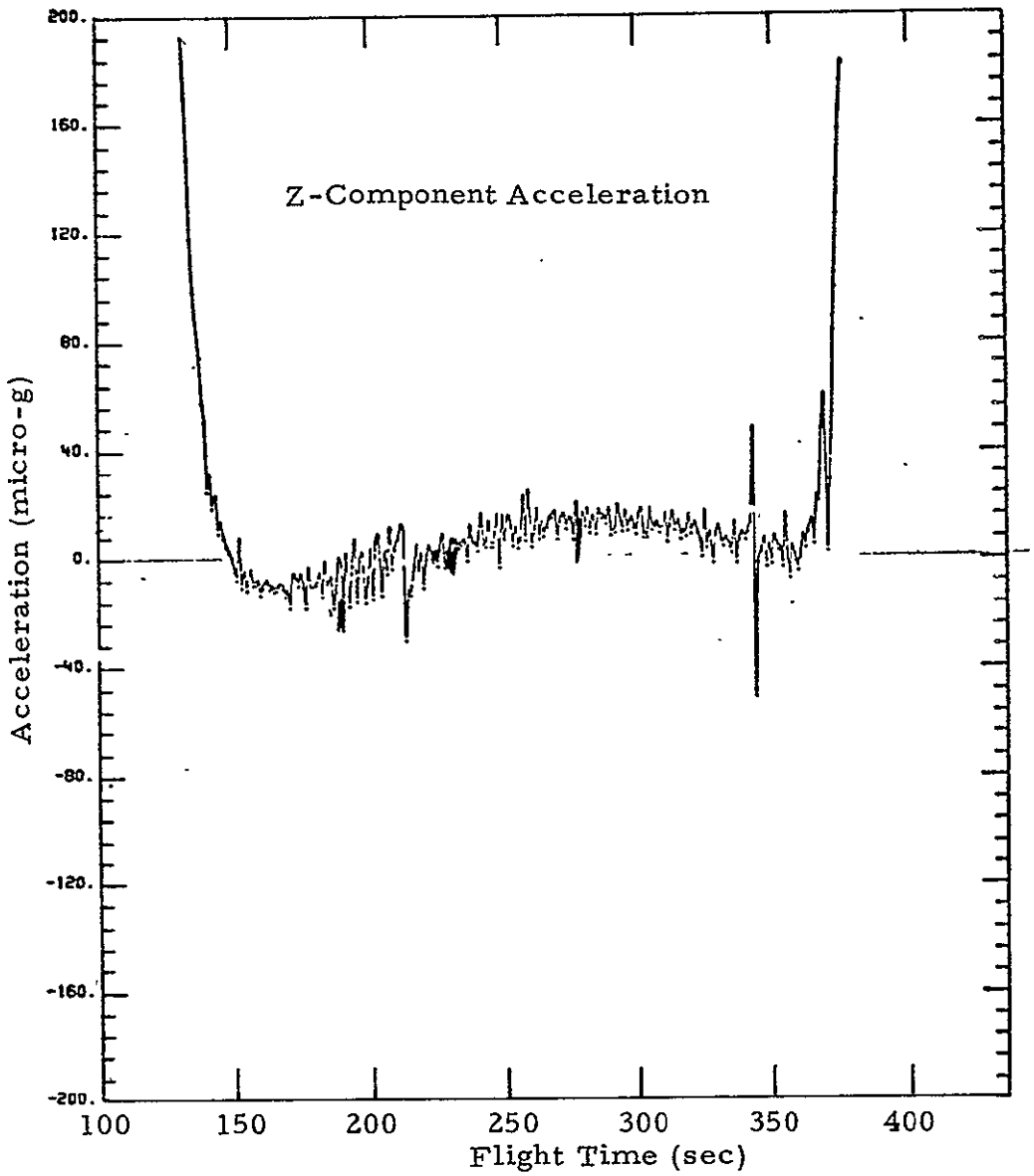

Fig. 5 - Gravity Level in Z Direction During Flight

3. RESIDUAL FLOW VELOCITIES AFTER DE-SPIN

In addition to convective fluid motions induced by gravity forces, some of the rotational velocities that existed during the spin-stabilized mode of rocket flight remain after de-spin occurs at 70 sec flight time. These velocities decay over a period of time due to dissipative viscous forces.

A number of spin-up and spin-down studies have been made for cylindrical containers, either full or with a free surface. A comprehensive review of studies prior to 1974 is given by Benton and Clark in Ref. 1. McLeod (Ref. 2) studied laminar flow spin-up and spin-down in circular cylinders where the effects of the end walls or free surfaces may be neglected. A recent analysis and comparison with experiment made by Weidman (Ref. 3 and 4) for spin-up and spin-down in circular cylinders includes the effects of end walls. In any event, the application of these studies to our rectangular containers will be useful for order-of-magnitude estimates only.

The dimensionless parameters of primary interest to spin-up and spin-down in circular cylinders are the Ekman and Reynolds numbers defined by

$$E = \frac{\nu}{\Omega h^2}$$
$$R_e = a\sqrt{\frac{\Omega}{\nu}} \qquad (1)$$

where ν is the kinematic viscosity, Ω is the rotational velocity, a is cylinder radius and h is cylinder height. We assumed that both a and h (effective cylinder dimensions) for our rectangular containers are of order 1 cm. For an initial spin-rate Ω = 240 rpm and kinematic voscosity $\nu = 9.3 \times 10^{-3}$ cm^2/sec for the ammonium chloride solution, the Ekman and Reynolds numbers E and R_e, respectively, are found to be $E = 3.88 \times 10^{-4}$ and $R_e = 50$.

Weidman's analysis is valid only for very small Ekman numbers ($<< 10^{-4}$ according to a recent telephone conversation with Weidman). Also, the side walls dominate for $E^{1/4} \sim 1$. In our case, $E^{1/4} = 0.14$, which is in the range where side walls should either be dominant or play a major role. Benton indicated in a 1975 telephone conversation that, where side walls dominate, the McLeod analysis should be used. The Reynolds number is low enough in our case that the flow is laminar (Ref. 4); thus, McLeod's analysis should be valid.

Residual velocities based on McLeod's theory are plotted in Fig. 6 as a function of flight time. The velocity was computed at a radial distance of one-half the cylinder radius. Note that, although the decay is extremely rapid, residual velocities greater than 0.01 cm/sec may be present until about 120 sec flight time.

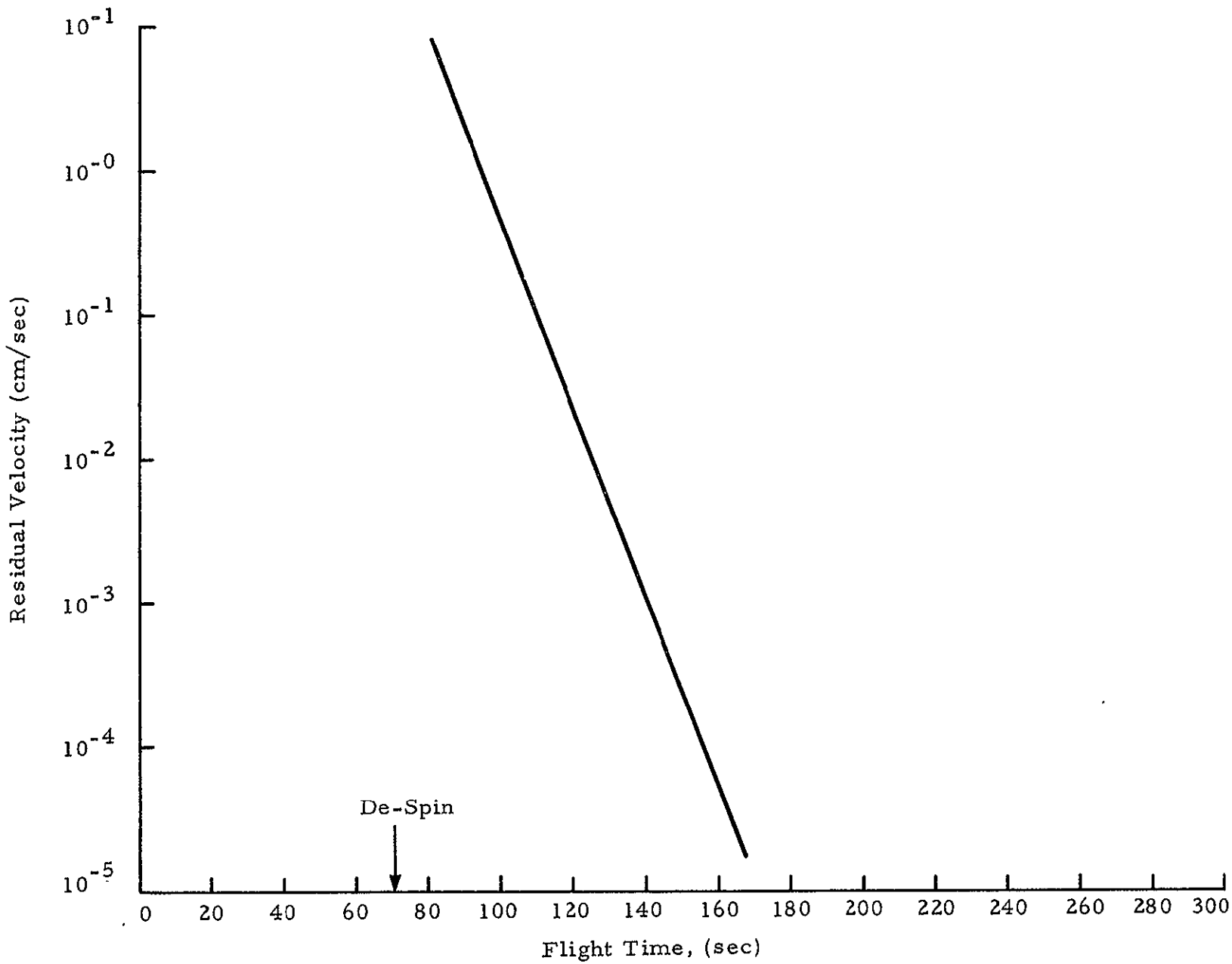

Fig. 6 - Residual Velocities After De-Spin (Estimated from Ref. 2)

4. THERMAL/CONVECTION ANALYSIS

Thermal analyses were performed to simulate heat transfer in the 74-21/2R and 74-21/3R experiment configurations during both flight and ground test. A Lockheed-Huntsville developed thermal analyzer computer code was used in these simulations. The experiment configurations, including both container and enclosed ammonium chloride solution, were modeled on the thermal analyzer program. Then the cooling rates where the thermoelectric devices contact the container surfaces were systematically adjusted until the temperatures at the thermistor locations satisfactorily matched the measured temperatures. The computed temperatures at the interface between the container and enclosed liquid were then used in an analysis of coupled thermal conduction and convection within the liquid.

4.1 RESULTS FOR 74-21/2R FLIGHT TEST

The measured temperatures at the T_1, T_2 and T_3 locations on experiment 74-21/2R are compared in Fig. 7 with the results of the thermal analyzer simulation. See Fig. 2 for the locations of the temperature measurements and the thermoelectric cooling device (TED). The "dip" in the measured data between 40 and 120 sec flight time is probably erroneous and, therefore, was ignored in the thermal analyzer simulation. Note that the thermal analyzer simulation results are in generally good agreement with the measured results at all three locations. The discrepancies may be due to several factors, including uncertainty in pinpointing the exact locations of the temperature measurements and error in thermal property data for the quartz container and ammonium chloride solution.

Thermal analyzer computed temperatures in the quartz container walls and in the enclosed liquid are shown in Fig. 8 for a section of container near the cooled face at various flight times. Note that the container wall is

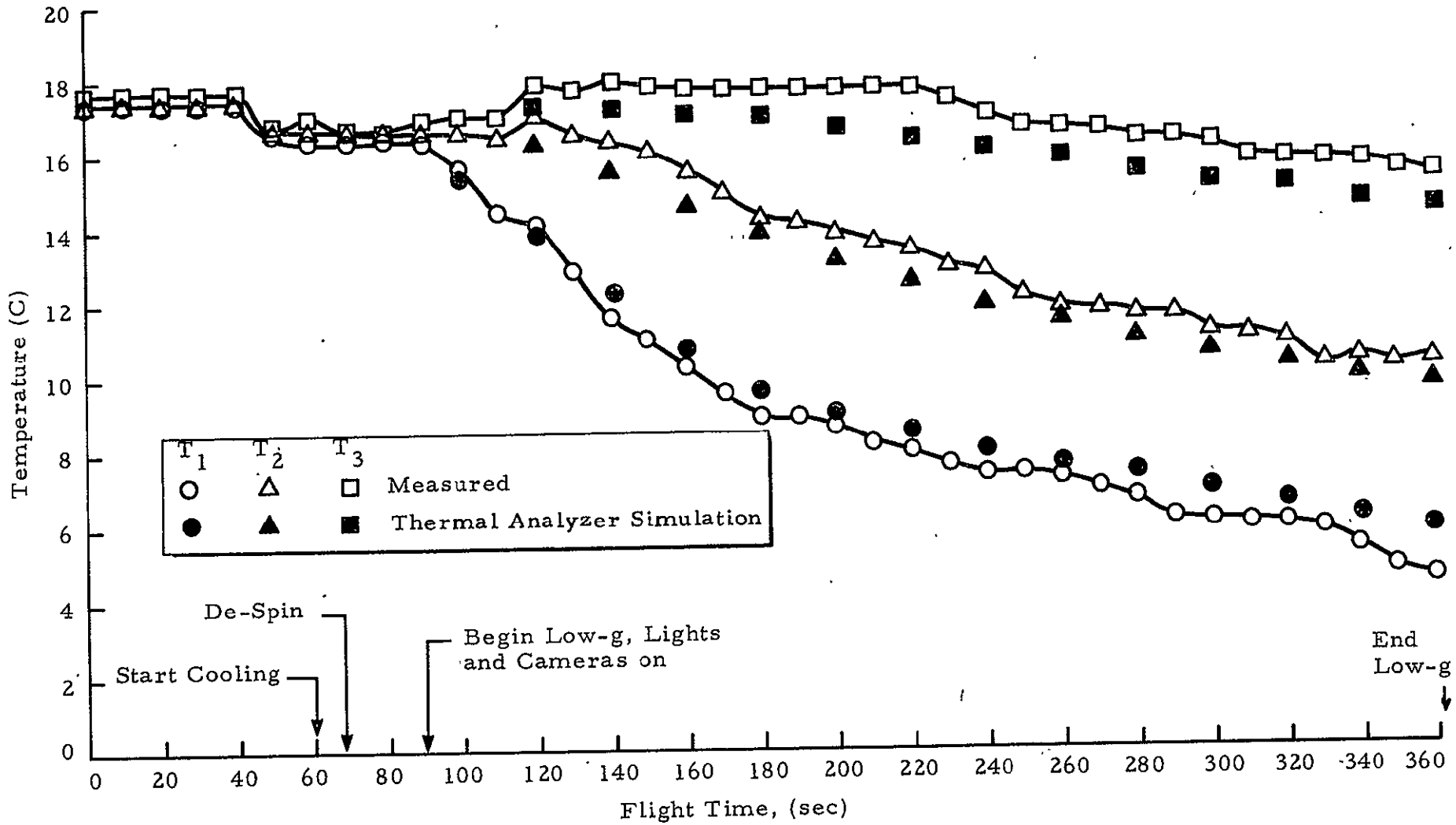

Fig. 7 - Measured Temperatures on 74-21/2R Flight Test Compared to Thermal Analysis Simulations

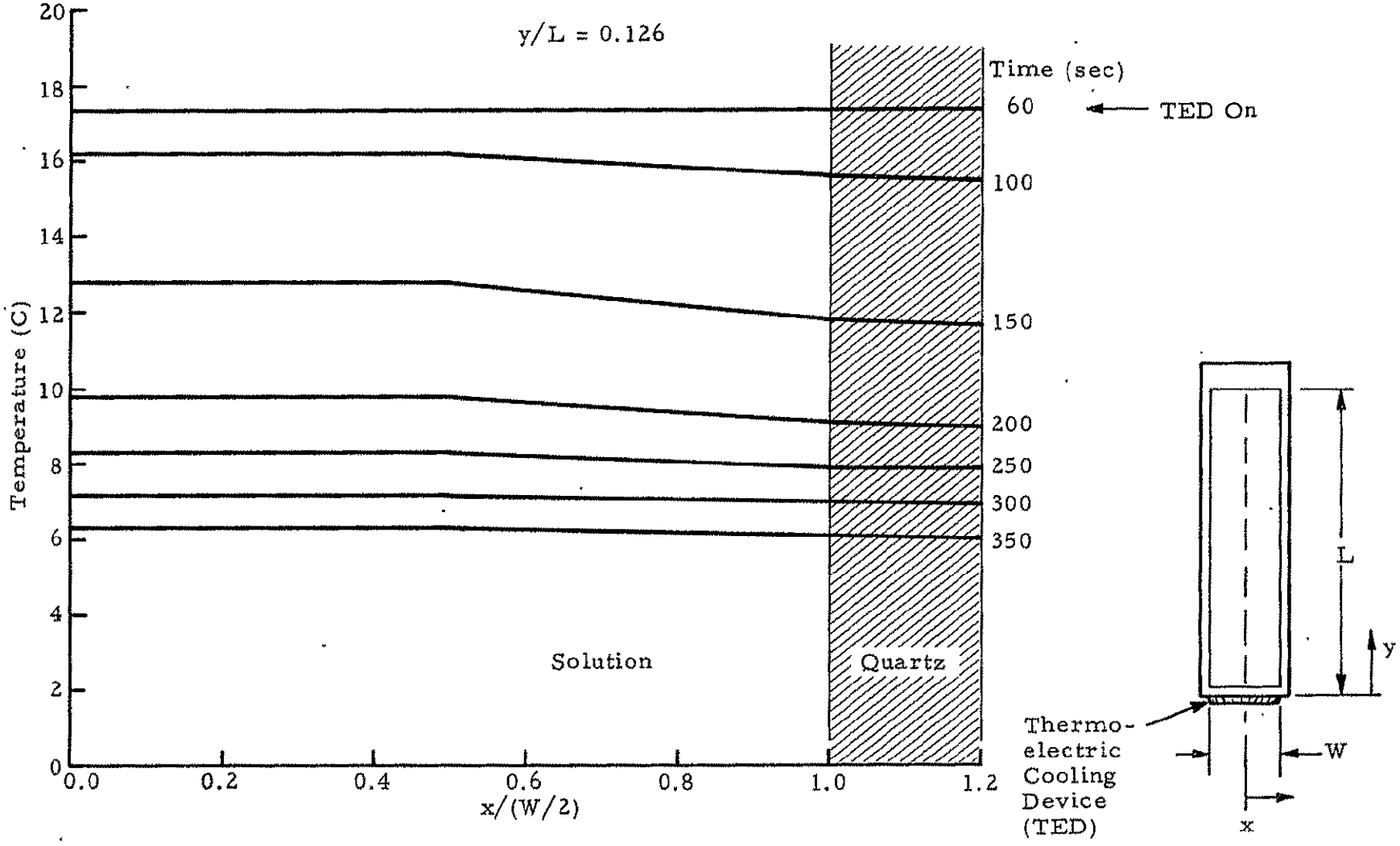

Fig. 8 - Thermal Analyzer Computed Temperatures in 74-21/2R Experiment at Various Times During Flight Test

substantially cooler than the enclosed liquid during the transient cool-down period. This is due to the higher thermal conductivity of the quartz material (3.3×10^{-3} cal/cm sec C) compared to the ammonium chloride solution (1.2×10^{-3} cal/cm sec C). The effect of the cooler walls will be to induce some side wall cooling of the liquid in addition to the expected longitudinal conduction toward the cooling surface.

The wall temperatures computed over the interior surface of the container by the thermal analyzer program were used as boundary conditions for the LOCAP two-dimensional coupled thermal conduction and convection analyzer code.

In the 74-21/2R experiment the +Y vehicle coordinate corresponds to the direction of the long (4 cm) container dimension and the +X vehicle coordinate corresponds to the 1-cm dimension. The camera views in the direction of the vehicle Z- axis through the 1/2 cm container dimension. The X and Y component accelerometer data shown in Figs. 3 and 4 were analytically modeled by the following Eqs. (2) and (3) to simulate the variation in gravity level over the experiment duration.

$$\begin{aligned} g_x = & -20 \times 10^{-6} (t - 90)/150 \\ & + 8 \times 10^{-6} \cos [2\pi (t - 90)/100] \\ & + 6 \times 10^{-6} \cos [2\pi (t - 90)/4] \end{aligned} \tag{2}$$

$$\begin{aligned} g_y = & 24 \times 10^{-6} - .0539 \times 10^{-6} (t - 90) \\ & + 10 \times 10^{-6} \cos [2\pi (t - 90)/157] \\ & + 6 \times 10^{-6} \cos [2\pi (t - 90)/4] \end{aligned} \tag{3}$$

These equations simulate fairly accurately the variation in average gravity level over the period of low-g flight. The high frequency variations are simulated by the superposition of the third term in the equations.

Using the temperature boundary conditions obtained from the thermal analyzer program and the gravity conditions simulated by Eqs. (3) and (4), temperature, density and velocity distributions were computed throughout the liquid as a function of flight time. As expected for the very low gravity conditions, the computed convective velocities were very low, the largest being on the order of 10^{-5} cm/sec. Heat transfer within the liquid, therefore, was essentially by conduction only. Computer generated plots of isotherms, streamlines and velocities are given in Fig. 9 at 10, 20, 50, 100, 200 and 300 sec after initiation of cooling at 60 sec flight time. The X and Y dimensions on the computer plots are the short and long container dimensions, respectively. These plots show contours at intervals of one-tenth the difference between extreme values and are intended for a broad indication of gradients and flow patterns. Note that the isotherms are curved near the side walls to indicate side wall cooling as previously shown in Fig. 8. The streamline and velocity plots show an initial flow toward the cooling surface, probably due to thermal contraction of the liquid. Later on, circular flow patterns begin to develop, and, at the very low velocities computed, the convective flow results probably become meaningless.

A plot of centerline temperatures is shown in Fig. 10 as a function of distance from the cooling surface at various flight times. Note that the cooled region is confined to about 2 cm from the cooling surface, with the strongest variation in the region less than about 0.6 cm. The lateral variation in temperatures along a section 0.6 cm from the cooling surface is shown in Fig. 11 for various flight times. The strongest lateral gradients and, hence, sidewall cooling is indicated in the initial cool-down period between about 80 and 180 sec flight time. The longitudinal component of gravity is directed away from the cooling surface, and, therefore, is in the direction opposite the density gradient. For sufficiently high gravity levels, this would be unstable. From Fig. 10, the temperature gradient near the surface is seen to be nearly constant at about 10 C/cm during the first 100 sec of cool down. This corresponds to a nearly constant surface heat flux of about -.012 cal/cm^2 sec. From Ref. 5, temperature penetration by pure conduction is described by Eq. (5) for a constant surface heat flux:

TIME = 10.0 (70 sec Flight Time)

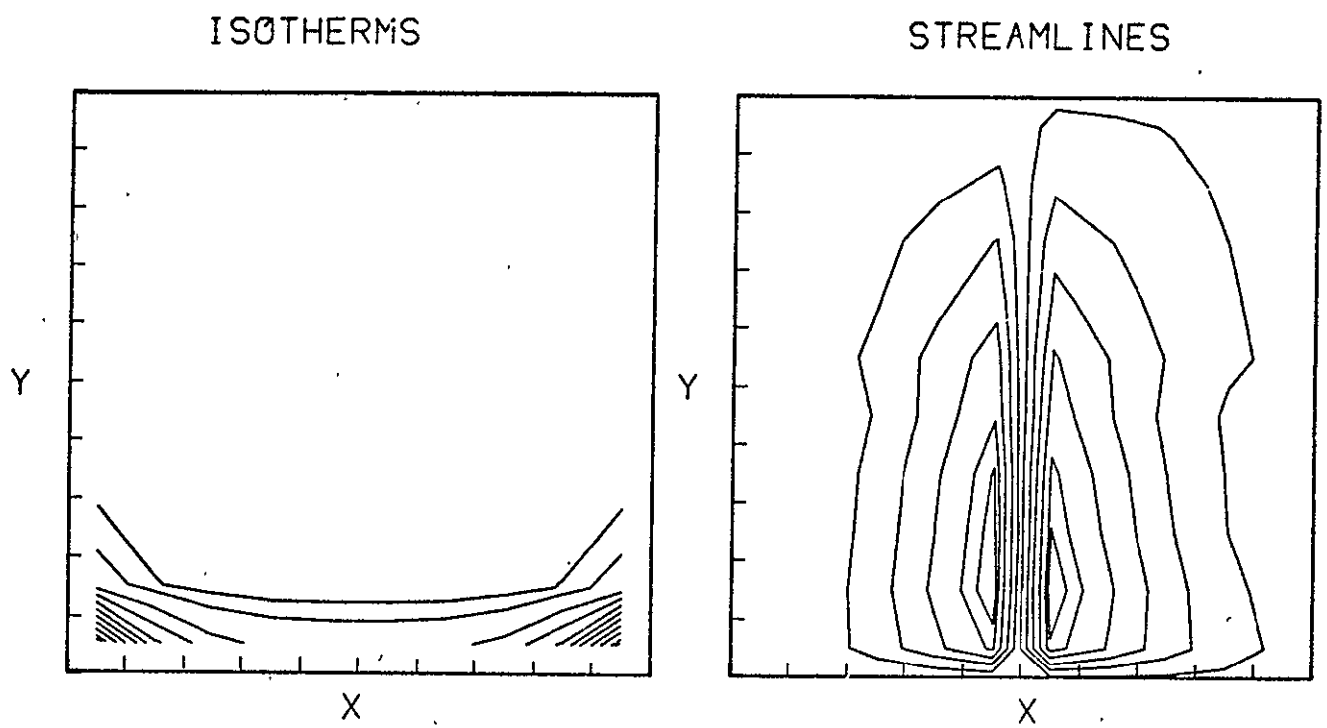

SPAR 74/21/2R FLIGHT TEST

Fig. 9 - Computer Generated Plots of Isotherms, Streamlines and Velocities for 74-21/2R Flight Test for Various Flight Times (Continued Next 11 Pages).

TIME = 10.0 (70 sec Flight Time)

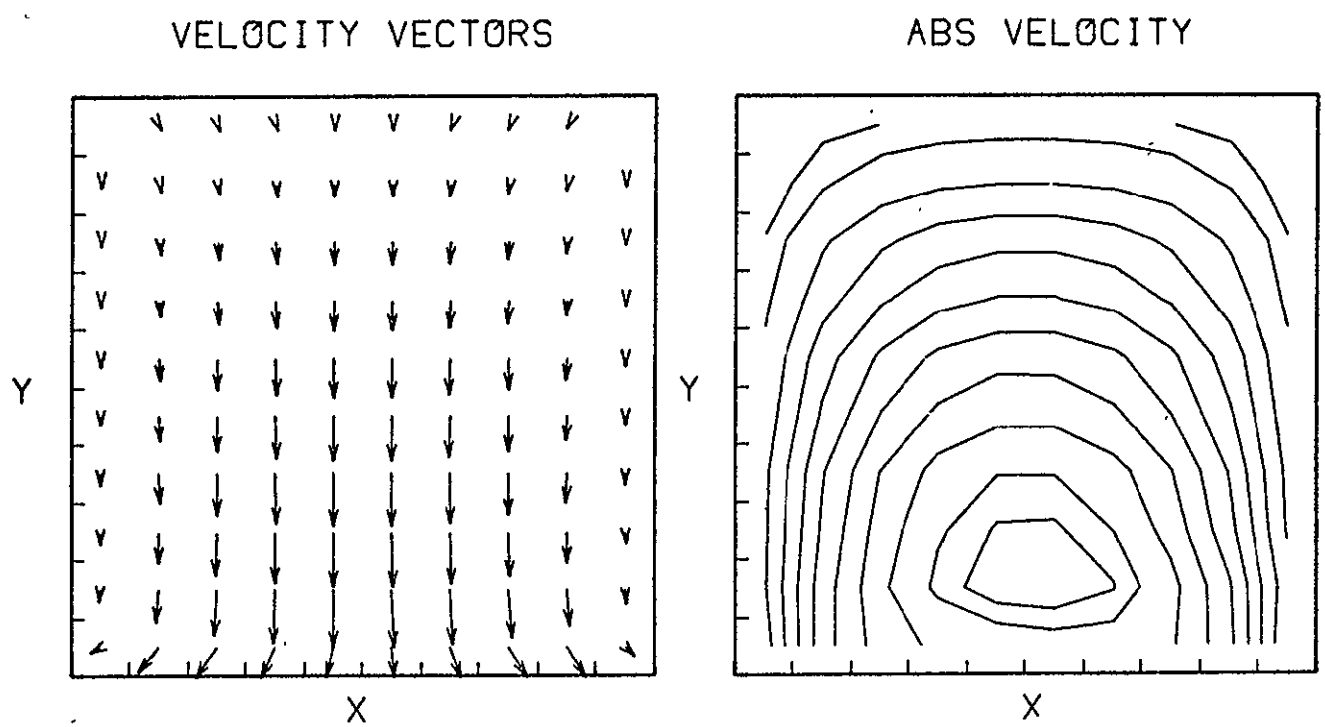

SPAR 74/21/2R FLIGHT TEST

Fig. 9 - Continued

TIME = 20.0 (80 sec Flight Time)

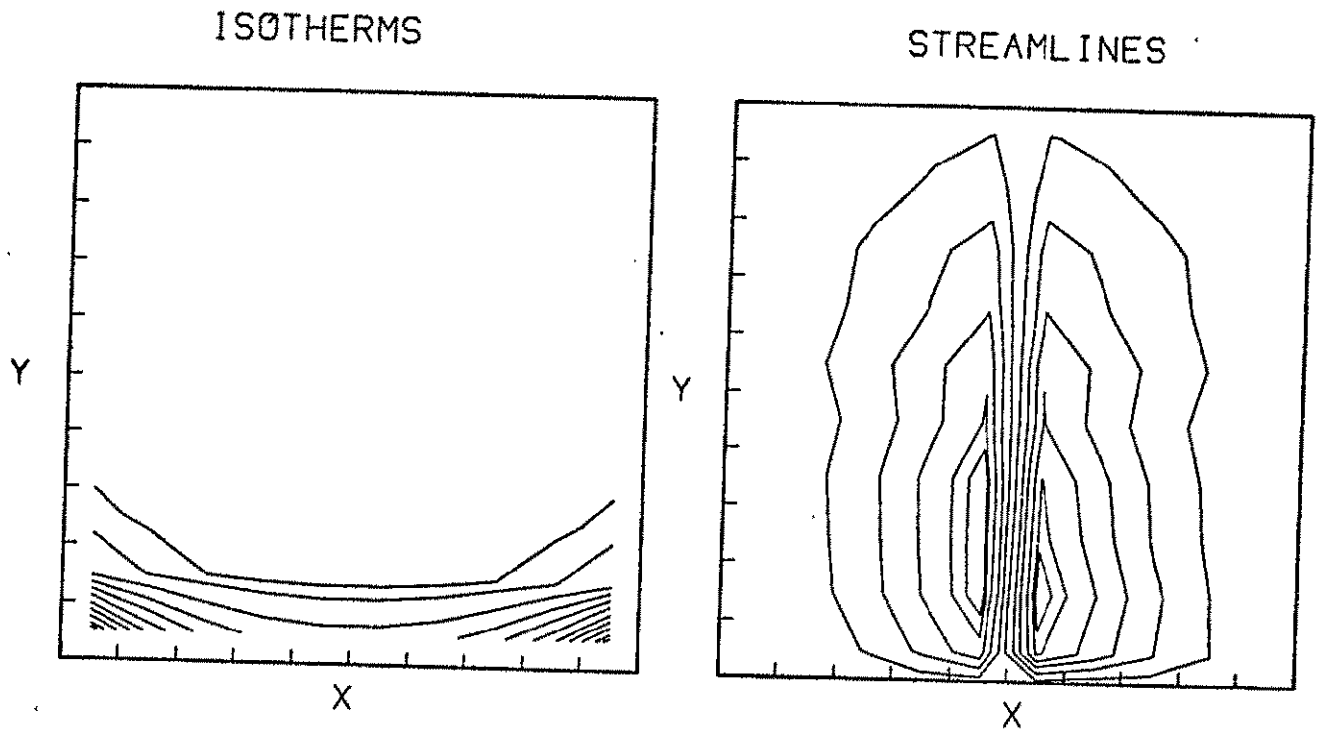

SPAR 74/21/2R FLIGHT TEST

Fig. 9 - Continued

TIME = 20.0 (80 sec Flight Time)

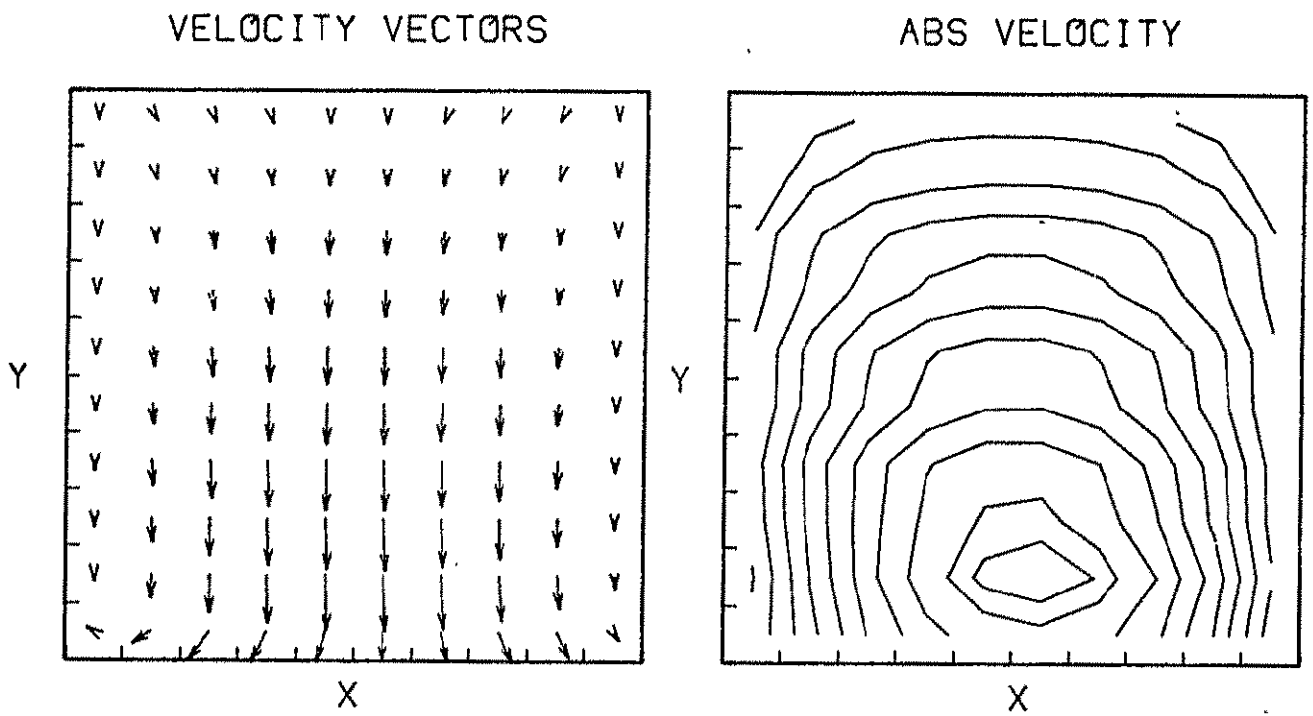

SPAR 74/21/2R FLIGHT TEST

Fig. 9 - Continued

TIME = 50.0 (110 sec Flight Time)

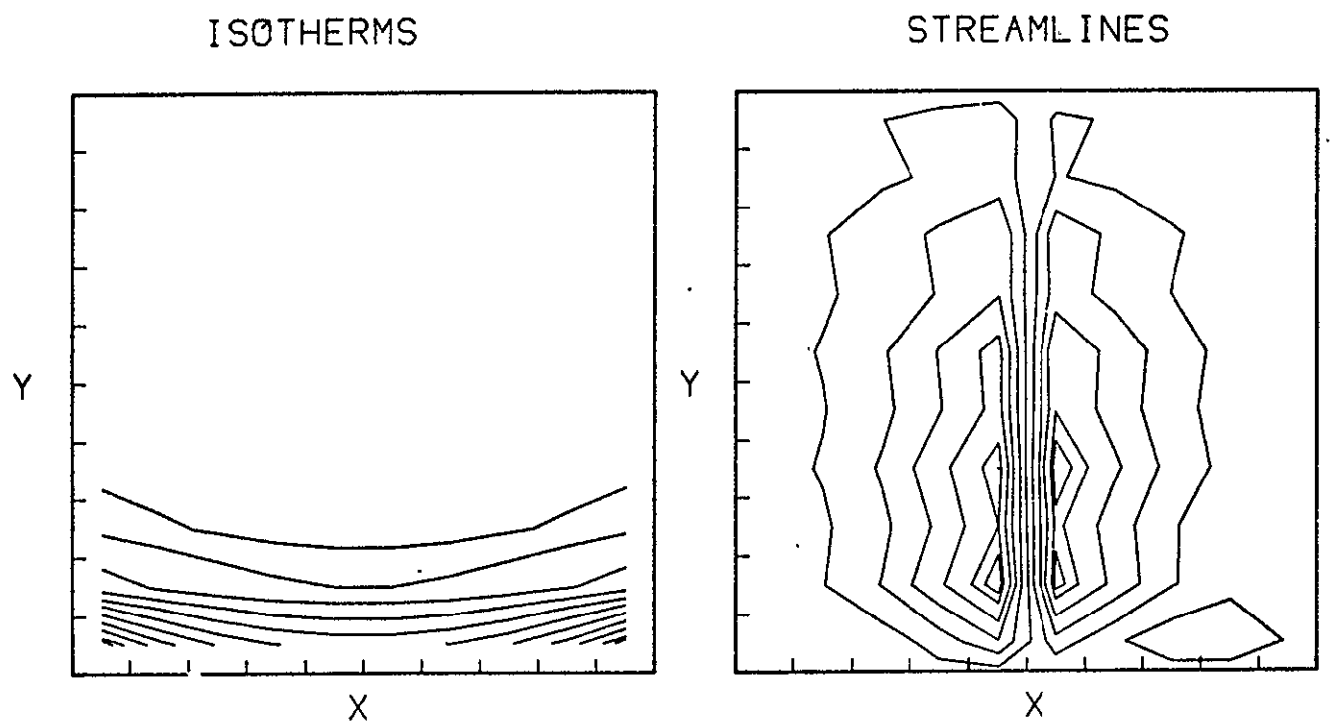

SPAR 74/21/2R FLIGHT TEST

Fig. 9 - Continued

TIME = 50.0 (110 sec Flight Time)

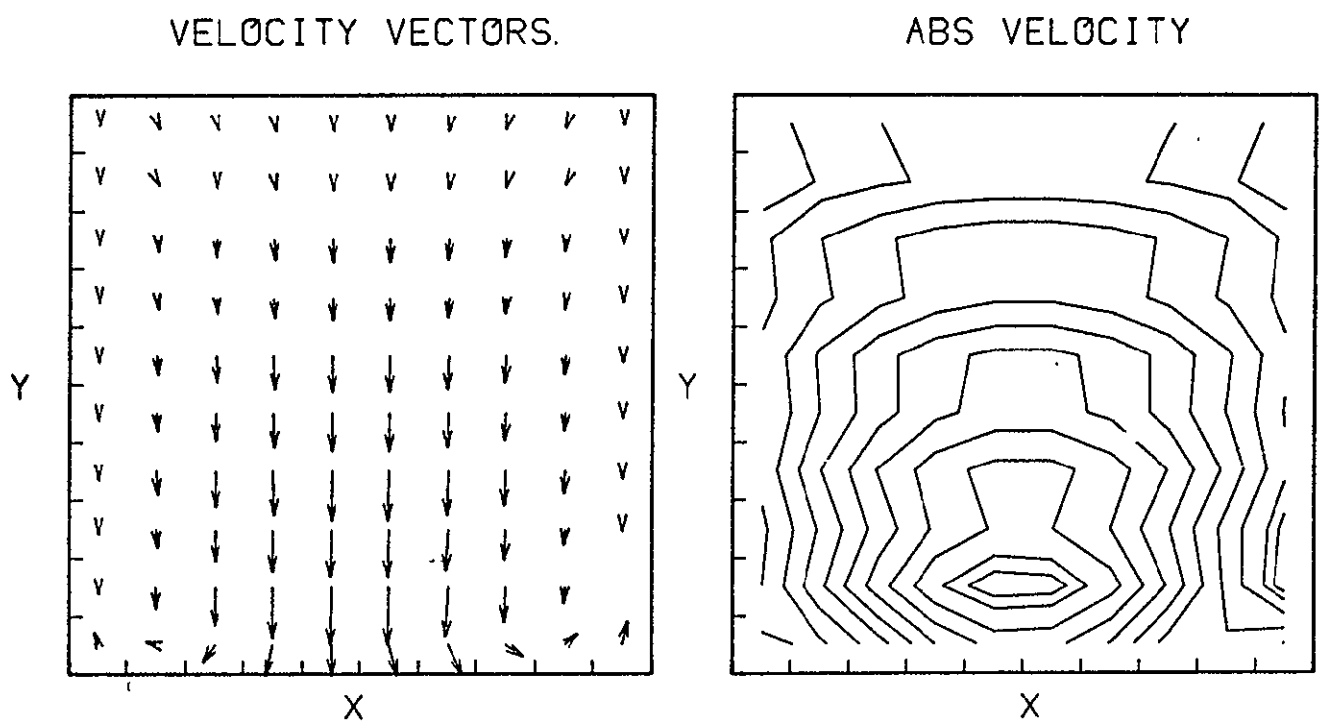

PAR 74/21/2R FLIGHT TEST

Fig. 9 - Continued

TIME = 100.0 (160 sec Flight Time)

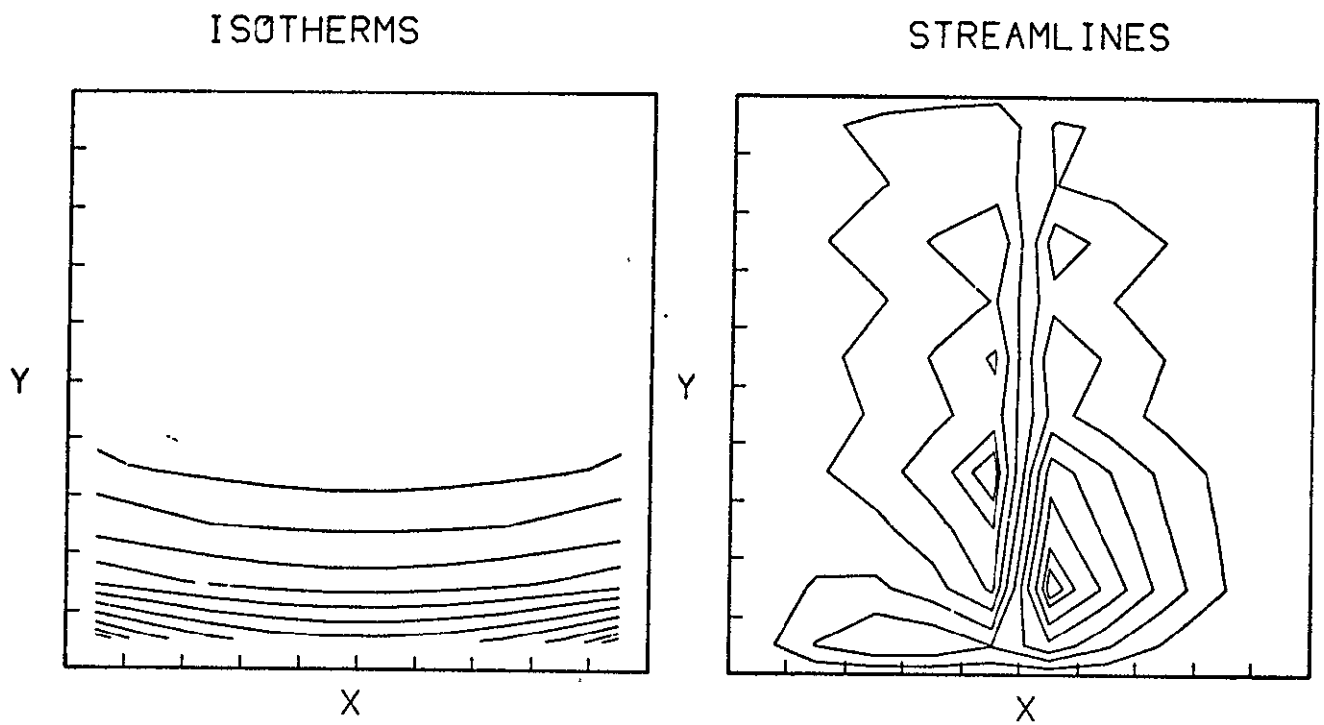

SPAR 74/21/2R FLIGHT TEST

Fig. 9 - Continued

TIME = 100.0 (160 sec Flight Time)

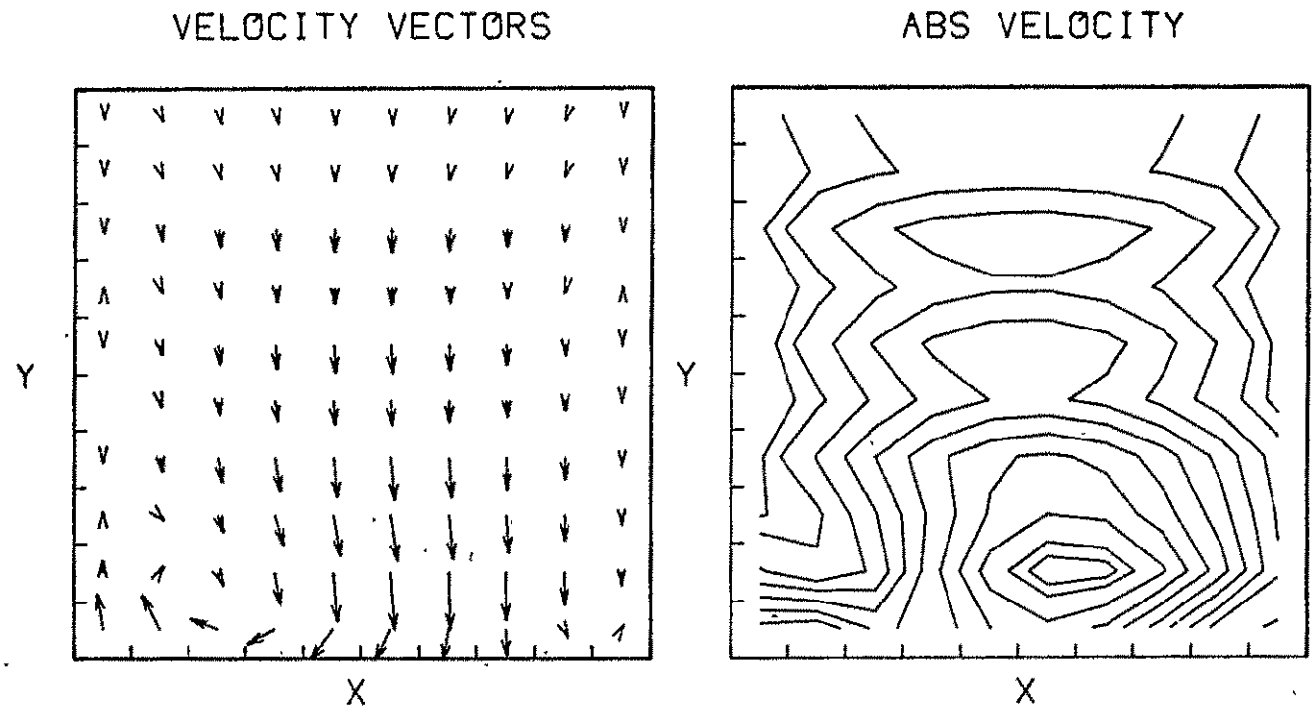

SPAR 74/21/2R FLIGHT TEST

Fig. 9 - Continued

TIME = 200.0 (260 sec Flight Time)

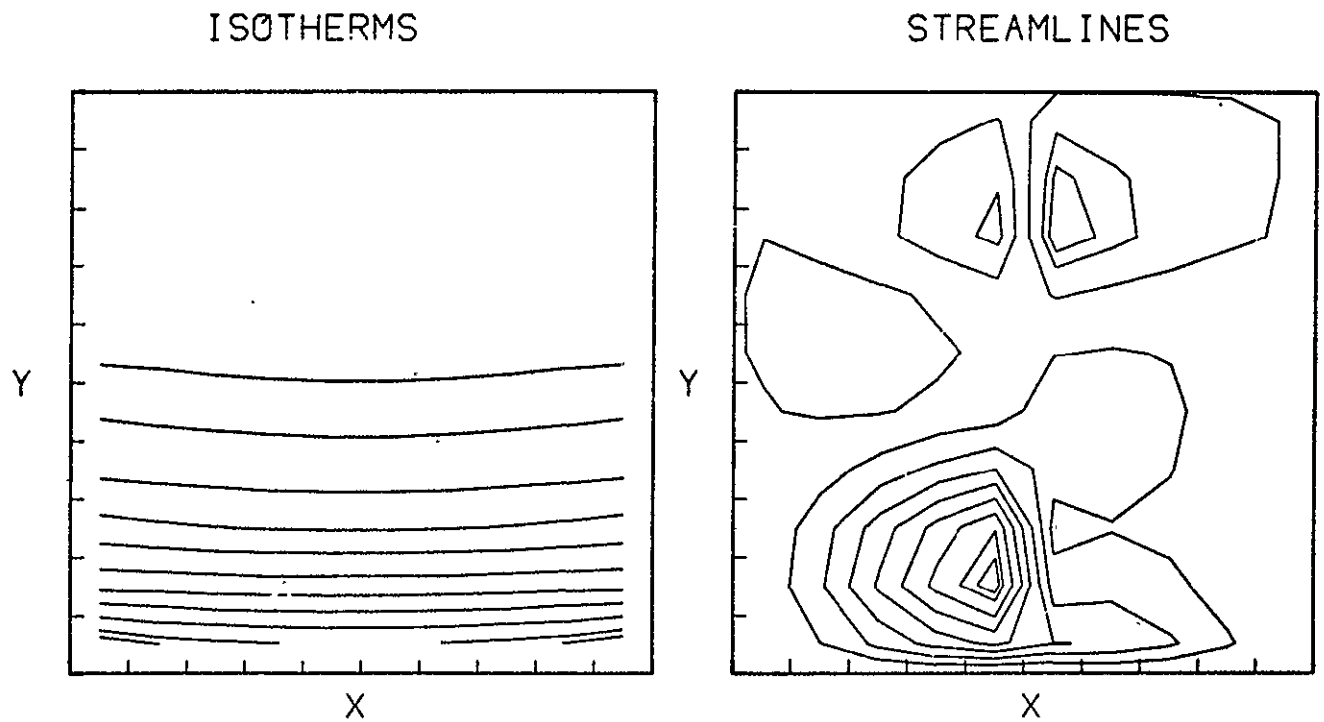

SPAR 74/21/2R FLIGHT TEST

Fig. 9 - Continued

TIME = 200.0 (260 sec Flight Time)

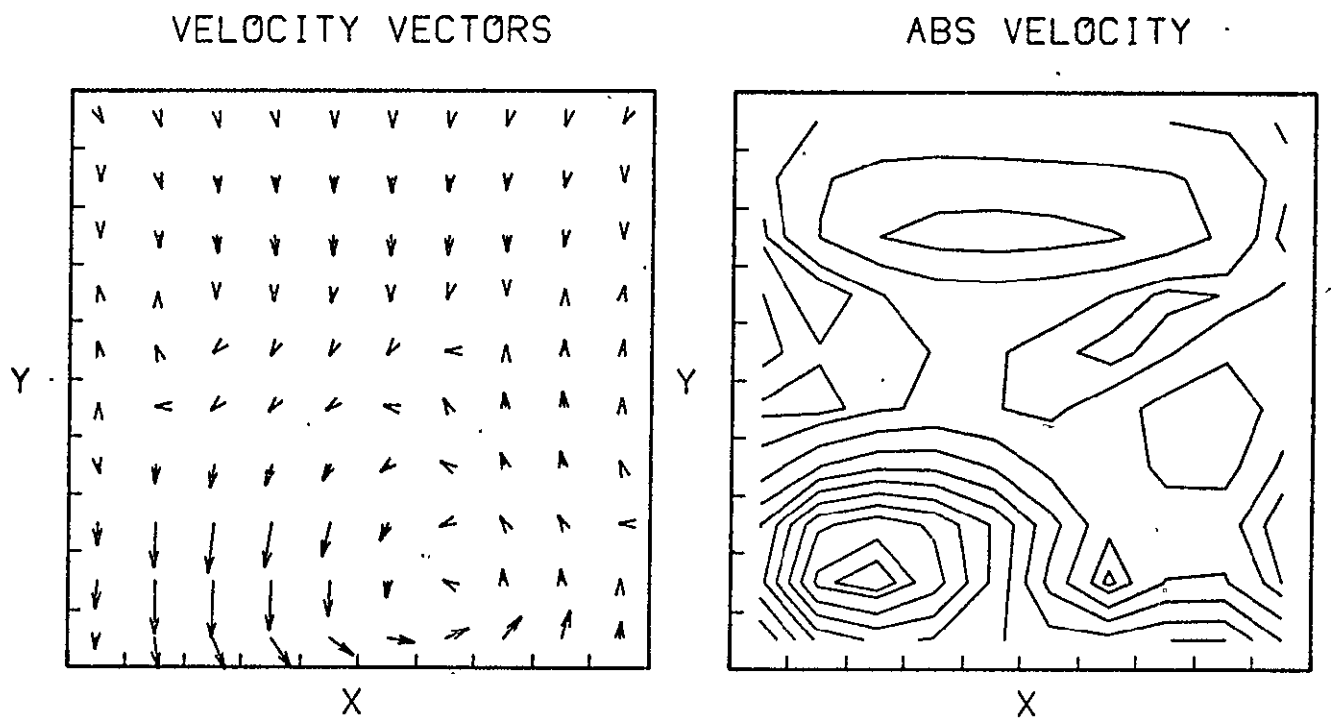

SPAR 74/21/2R FLIGHT TEST

Fig. 9 - Continued

TIME = 300.0 (360 sec Flight Time)

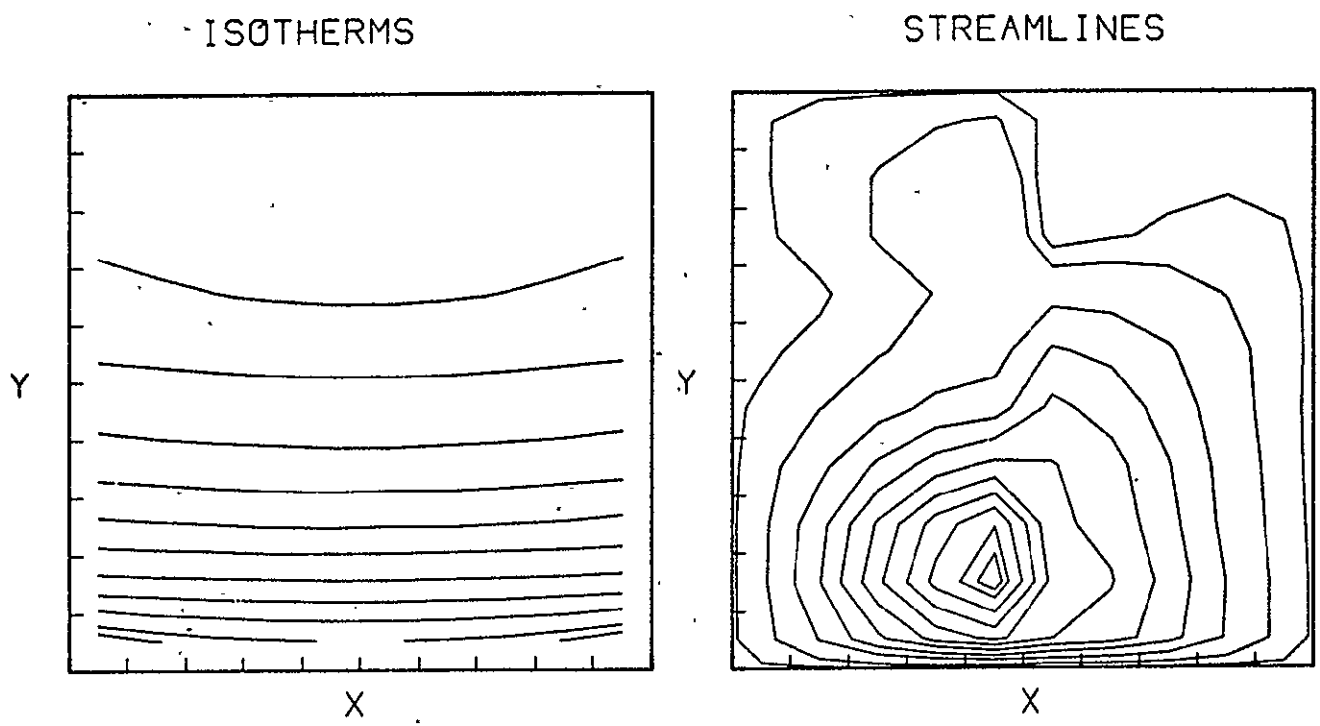

SPAR 74/21/2R FLIGHT TEST

Fig. 9 - Continued

TIME = 300.0 (360 sec Flight Time)

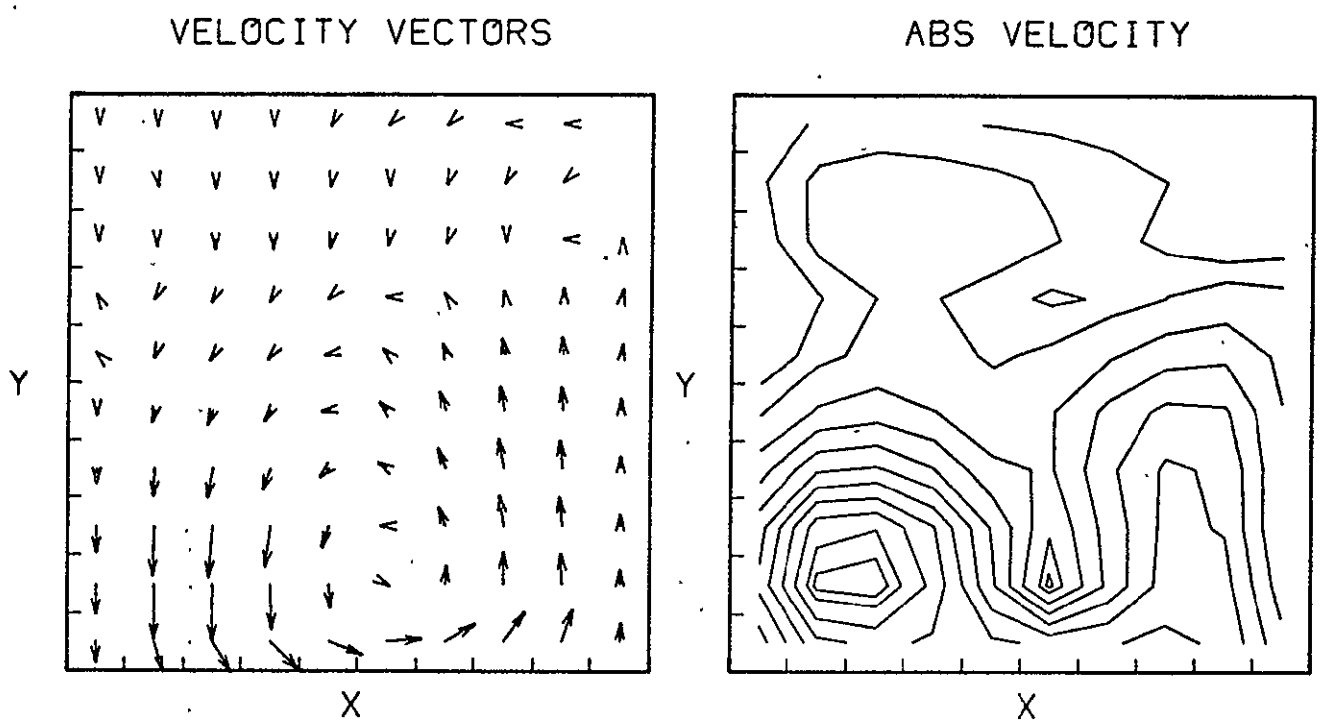

SPAR 74/21/2R FLIGHT TEST

Fig. 9 - Concluded

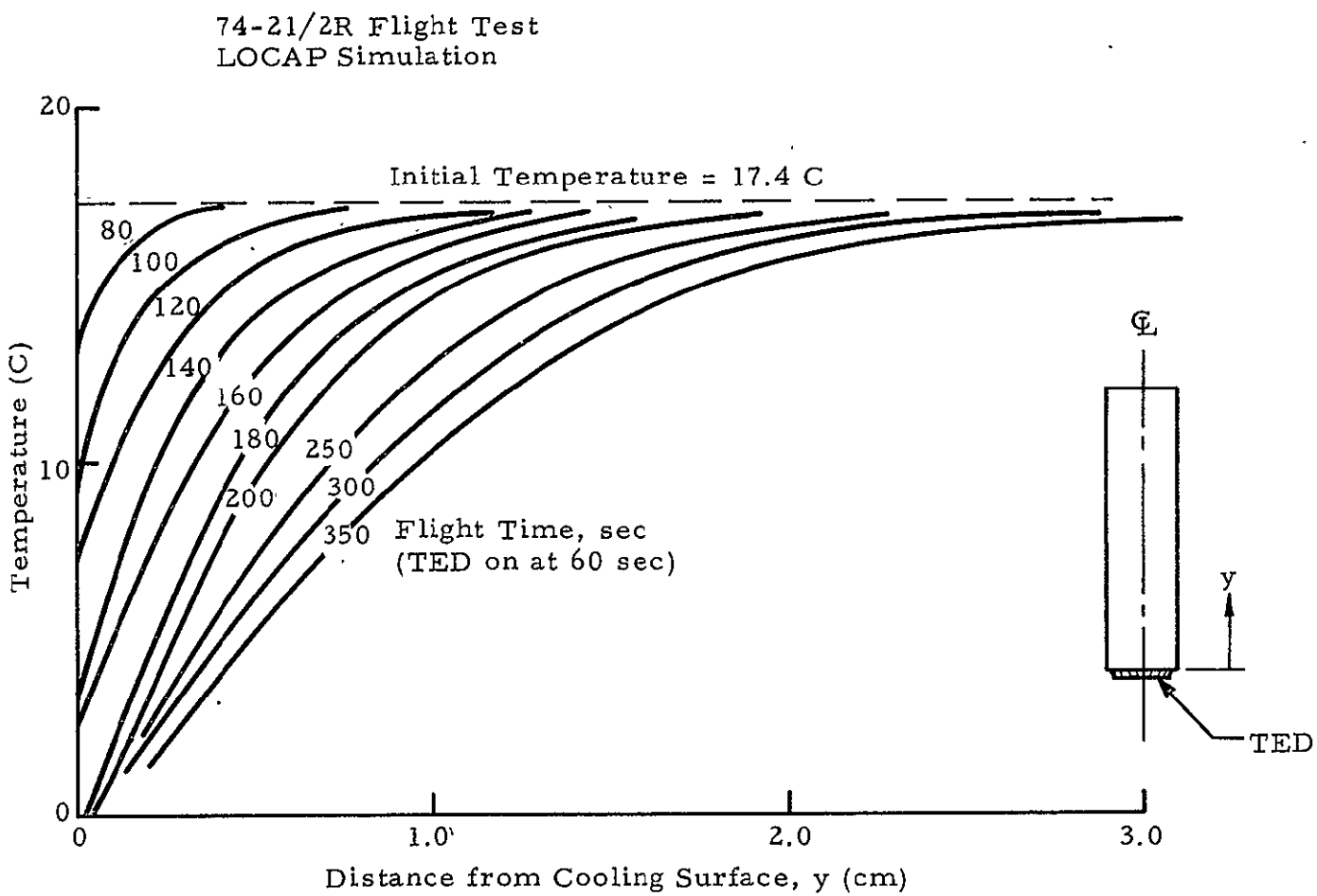

Fig.10 - Centerline Temperature Distributions for 74-21/2R Flight Test for Various Flight Times

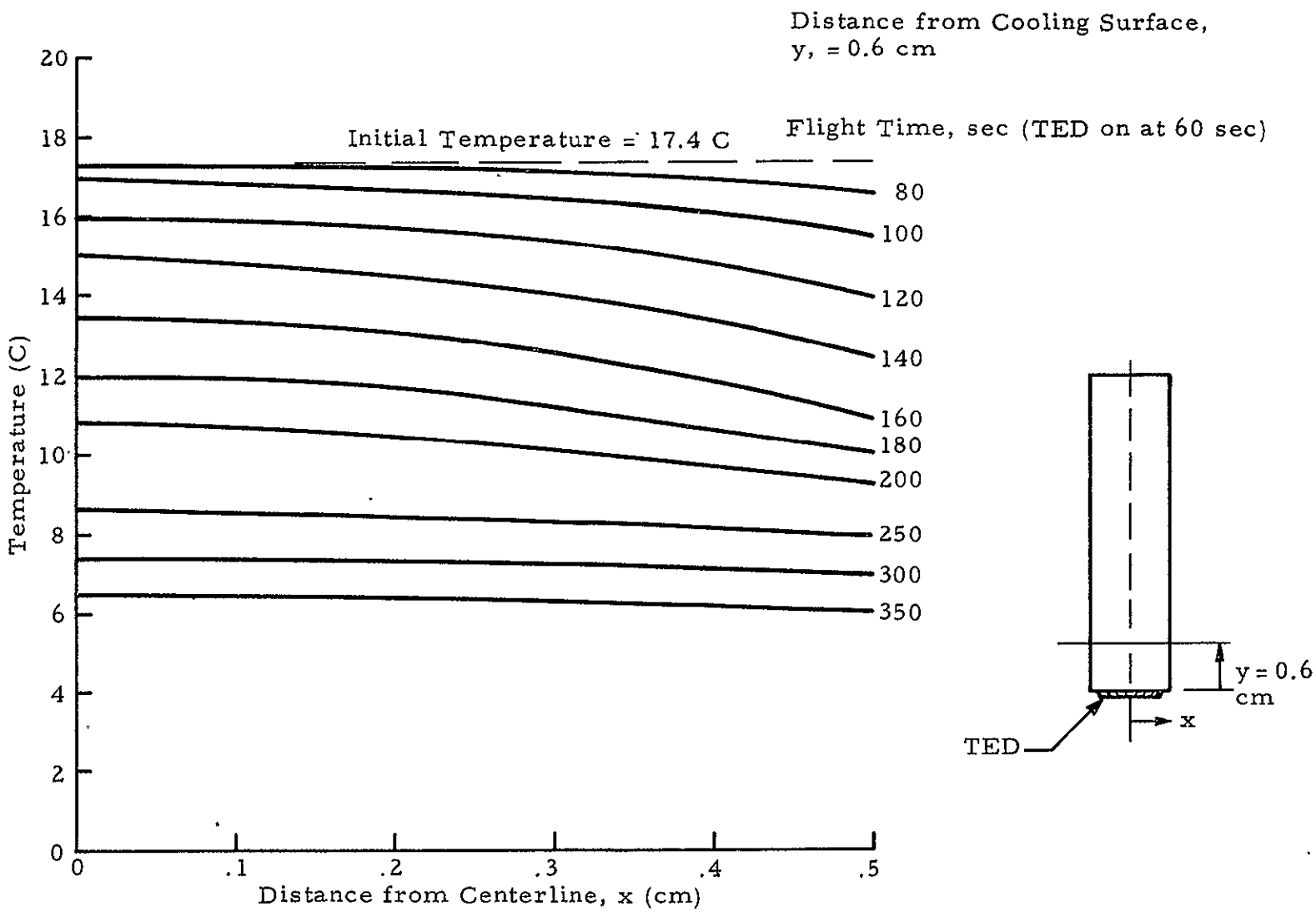

Fig. 11 - Lateral Temperature Distributions for 74-21/2R Flight Test for Various Flight Times

$$T(y, t) = T_o - \frac{2q\sqrt{\alpha t}}{k} \text{ ierfc } \frac{y}{2\sqrt{\alpha t}} \tag{4}$$

with the surface temperature being

$$T(o, t) = T_o - \frac{2q\sqrt{\alpha t}}{k} \tag{5}$$

where T is temperature, y is distance from the surface, t is time, q is surface heat flux, α is thermal diffusivity and k is thermal conductivity. From the shape of the ierfc function, a characteristic temperature penetration depth is given by

$$\delta \sim 2\sqrt{\alpha t} \tag{6}$$

From Eq. (6), the difference between the surface temperature and the undisturbed temperature at depth is

$$\Delta T = \frac{2q\sqrt{\alpha t}}{k} \tag{7}$$

Using Eqs. (6) and (7), effective thermal Rayleigh numbers Ra_T for this experiment configuration can be defined as:

$$\begin{aligned} Ra_T &= \frac{g\,\beta_T\,\Delta T\,\delta^3}{\nu\alpha} \\ &= \frac{16\,g\,\beta_T\,q}{\nu\,\rho\,C}\,t^2 \end{aligned} \tag{8}$$

where g is gravity level, β_T is the thermal expansion coefficient, ν is kinematic viscosity, ρ is density and C is specific heat. Using $g = 2 \times 10^{-5}$ g_E (.02 cm/sec^2), $\beta_T = 2.95 \times 10^{-4}$/C, q = .012 cal/cm^2 sec, $\nu = 9.3 \times 10^{-3}$ cm^2/sec, $\rho = 1.08$ g/cm^3 and C = .74 cal/g C, Eq. (8) becomes

$$Ra_T = 1.5 \times 10^{-4}\,t^2 \text{ (t in sec)} \tag{9}$$

The Rayleigh number is seen to be only 1.5 at t = 100 sec after initiation of cooling (160 sec flight time) and 14 at t = 300 sec (360 sec flight time). According to Ref. 6, convective flow should not be initiated for Rayleigh numbers less than about 1000. The 74-21/2R flight test experiment, therefore, should be stable from the standpoint of thermally driven convection.

4.2 RESULTS FOR 74-21/3R FLIGHT TEST

The measured temperatures at the T_4, T_5, T_6 and T_7 locations on experiment 74-21/3R are compared in Figs. 12 through 15 with the results of the thermal analyzer simulation. As shown in Fig. 2, the temperature measurements at T_4, T_5 and T_7 were located adjacent to thermoelectric cooling devices on faces being cooled. The thermal analyzer simulation therefore entailed adjusting the surface cooling rates until temperatures computed at the T_4, T_5 and T_7 locations satisfactorily matched the measurements. The T_6 measurement was located midway between the two cooled surfaces on which the T_4 and T_5 measurements were made. The thermal analyzer simulation indicated that a considerable lag should have been noted in the cooling at T_6 compared to that at T_4 and T_5. Unfortunately, the T_6 measurement closely followed the T_4 and T_5 measurements and failed to compare well with the thermal analyzer simulation. No explanation is available at this time. Possibilities include a thermal or electrical short between the T_6 and T_4 or T_5 measurements.

As with the 74-21/2R flight test data, the thermal analyzer computed interior container wall surfaces were used as boundary conditions in the LOCAP program. The X-component accelerometer data in Fig. 3 are in the direction of the long (4 cm) container dimension (positive in the direction toward the cooled 1 cm x 1 cm surface), and the Y-component (Fig. 4 and Eq. (3) data) are in the direction of the container axis between the two cooled 1 cm x 4 cm surfaces. The resulting LOCAP generated plots of isotherms, streamlines and velocities are shown in Figs. 16. The X and Y experiment coordinates shown in Fig. 16 correspond to the Y and -X vehicle coordinates, respectively. The temperature measurements shown in Figs. 12, 13 and 15

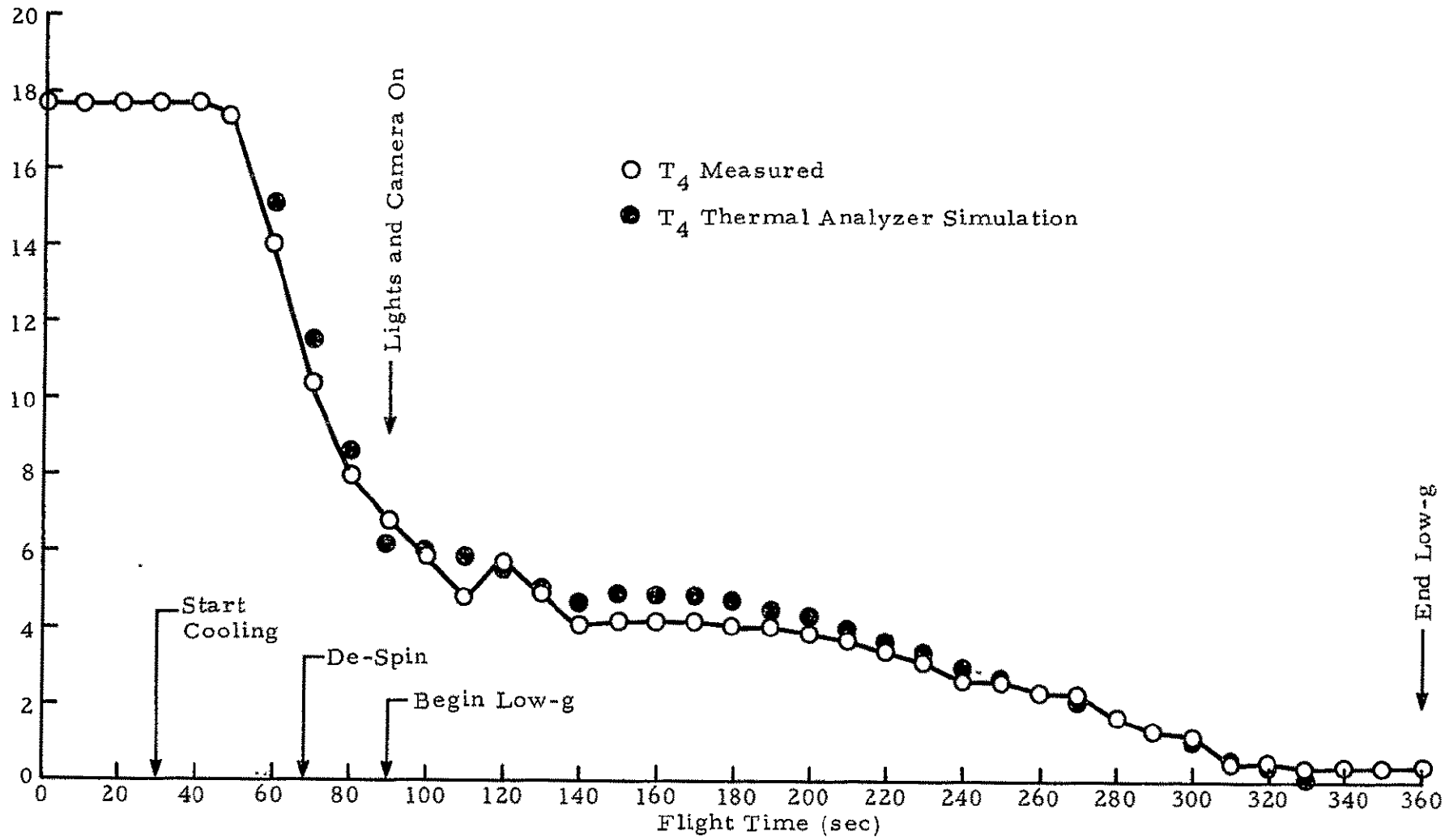

Fig. 12 - Measured Temperature at T_4 Location on 74-21/3R Flight Test Compared to Thermal Analyzer Simulation

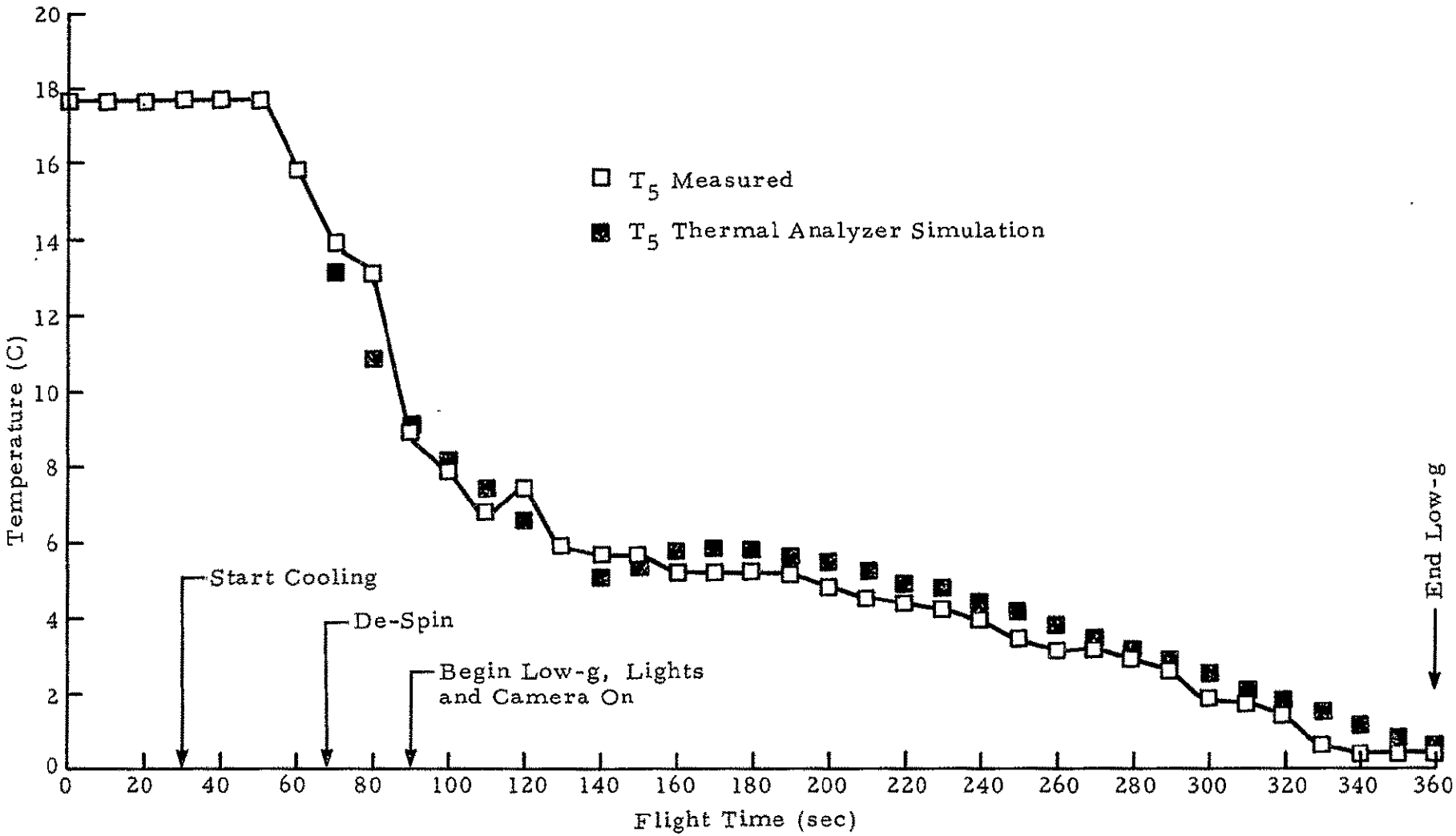

Fig. 13 - Measured Temperature at T_5 Location on 74-21/3R Flight Test Compared to Thermal Analyzer Simulation

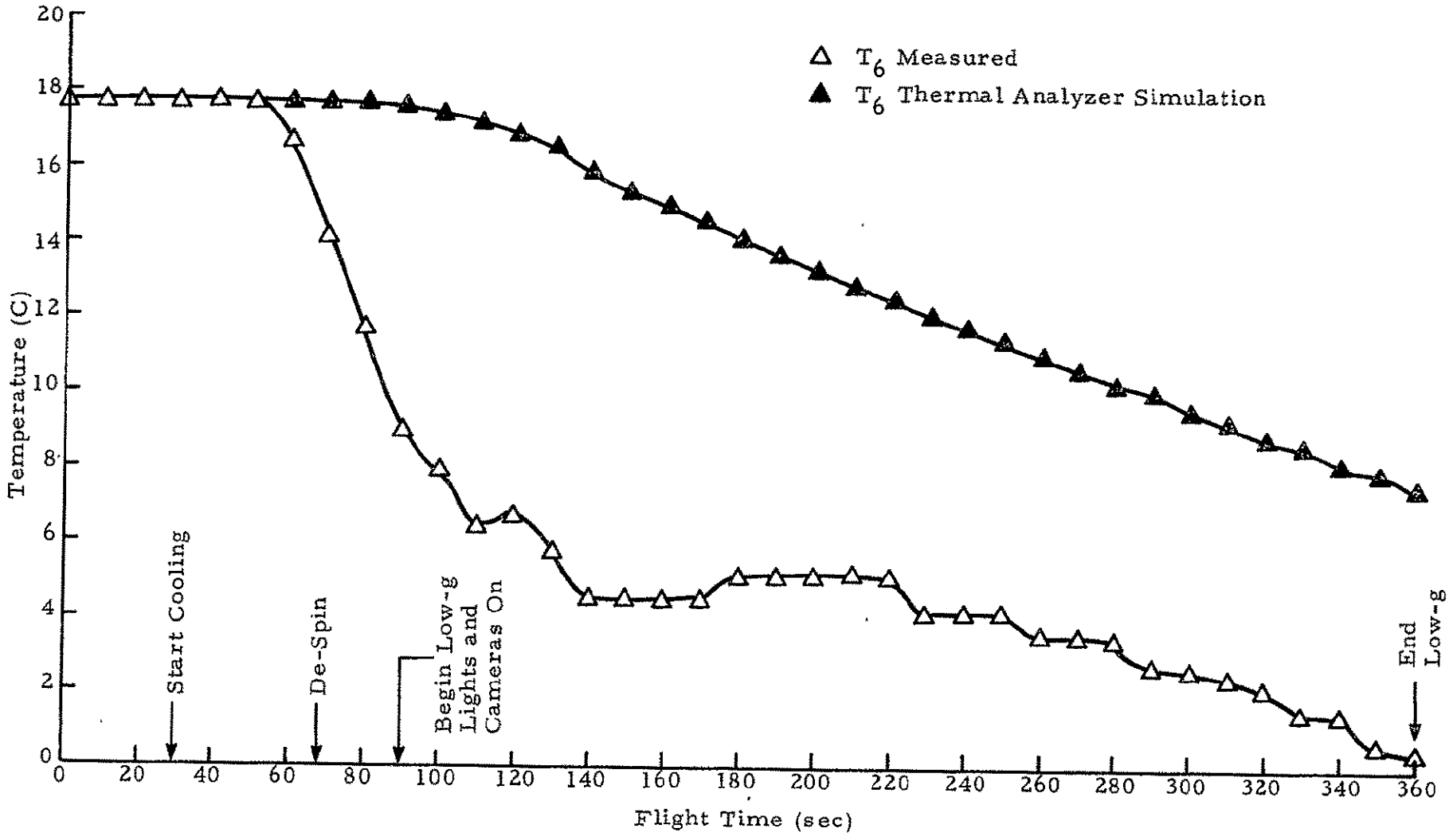

Fig.14- Measured Temperature at T_6 Location on 74-21/3R Flight Test Compared to Thermal Analyzer Simulation

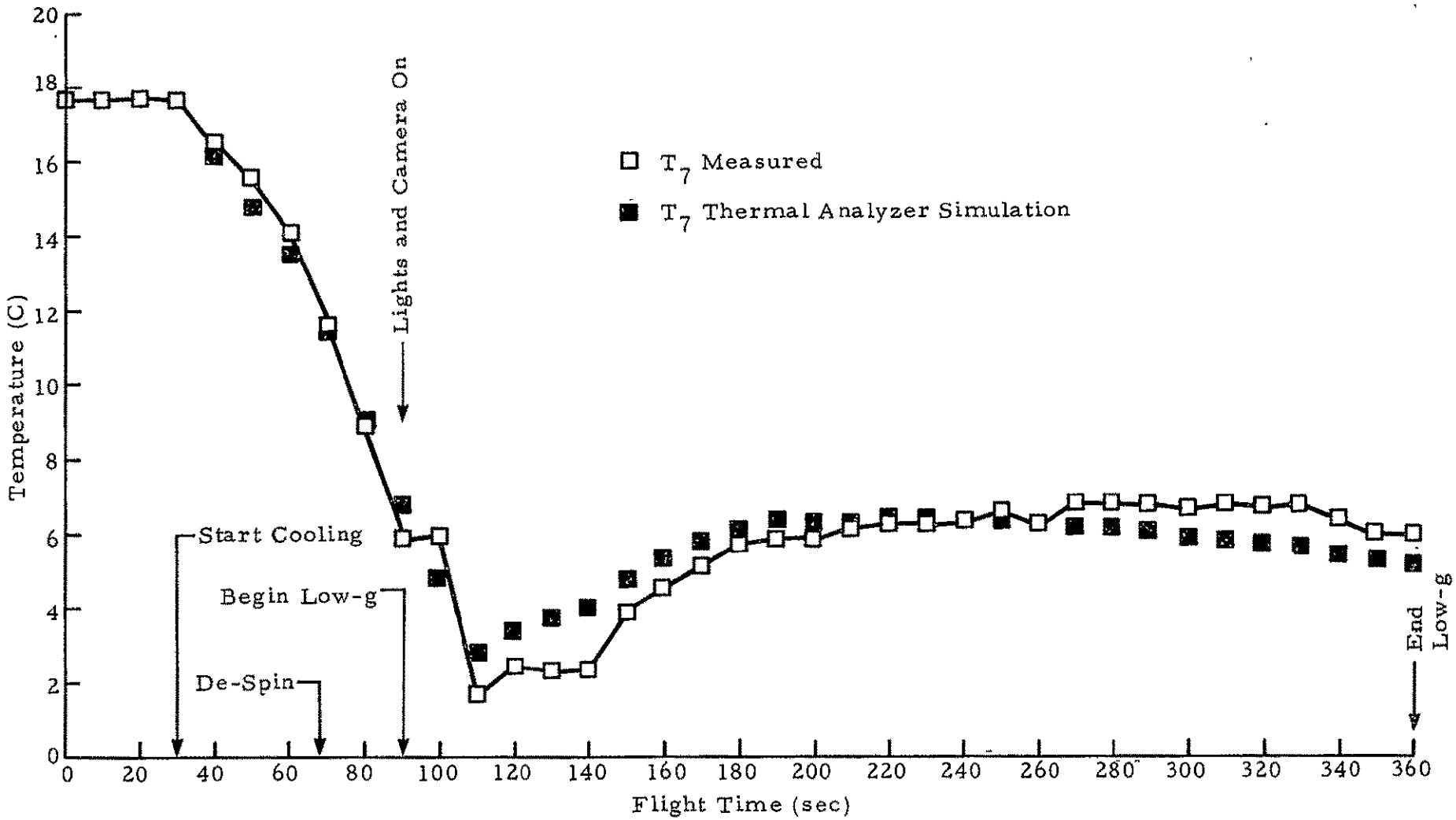

Fig. 15 - Measured Temperature at T_7 Location on 74-21/3R Flight Test Compared to Thermal Analyzer Simulation

TIME = 20.0 (50 sec Flight Time)

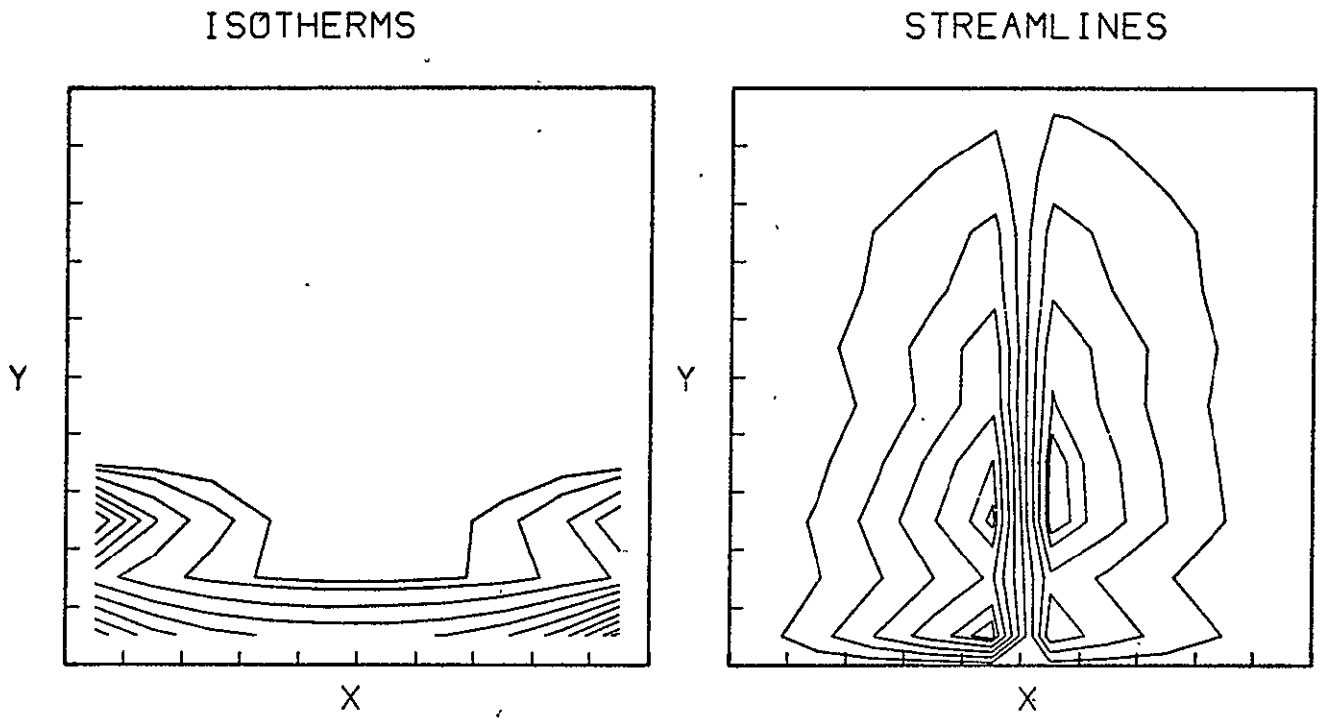

SPAR 74/21/3R FLIGHT TEST

Fig. 16 - Computer Generated Plots of Isotherms, Streamlines and Velocities for 74-21/3R Flight Test for Various Flight Times (Continued next 17 pages)

TIME = 20.0 (50 sec Flight Time)

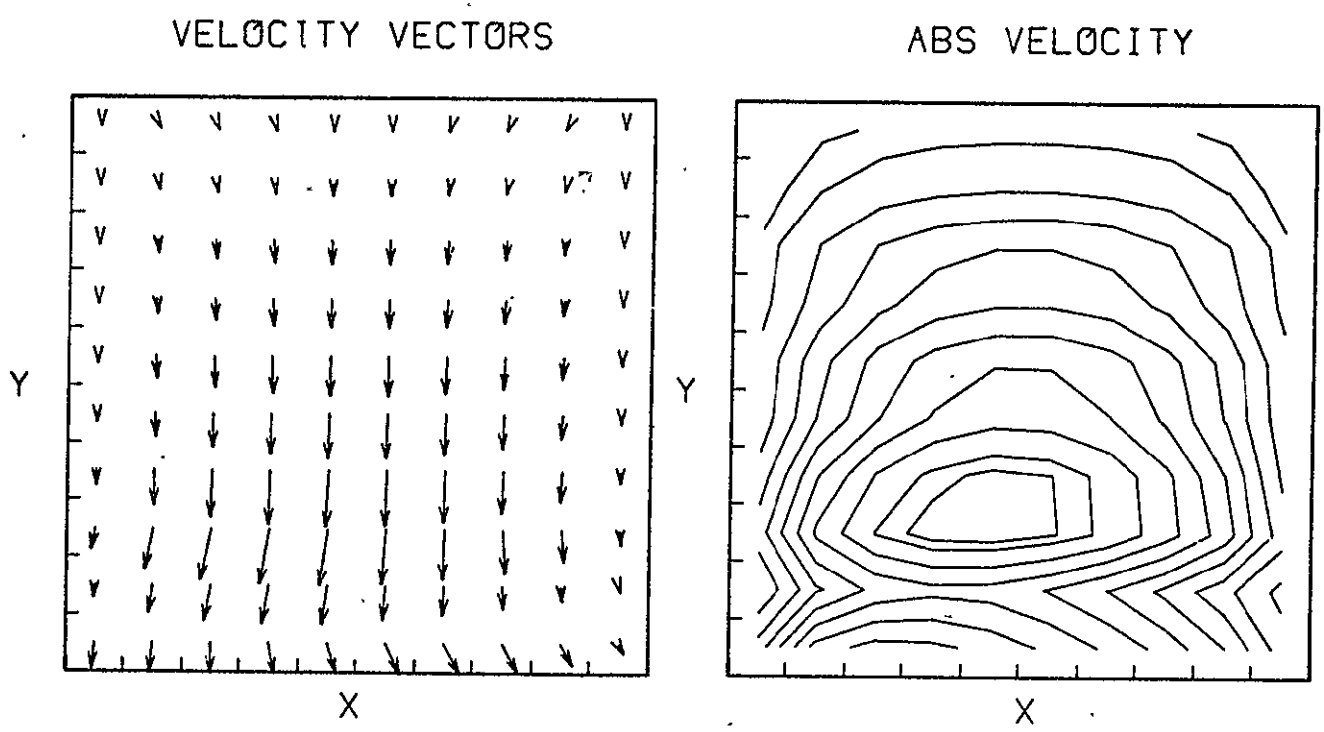

SPAR 74/21/3R FLIGHT TEST

Fig. 16 - Continued

TIME = 40.0 (70 sec Flight Time)

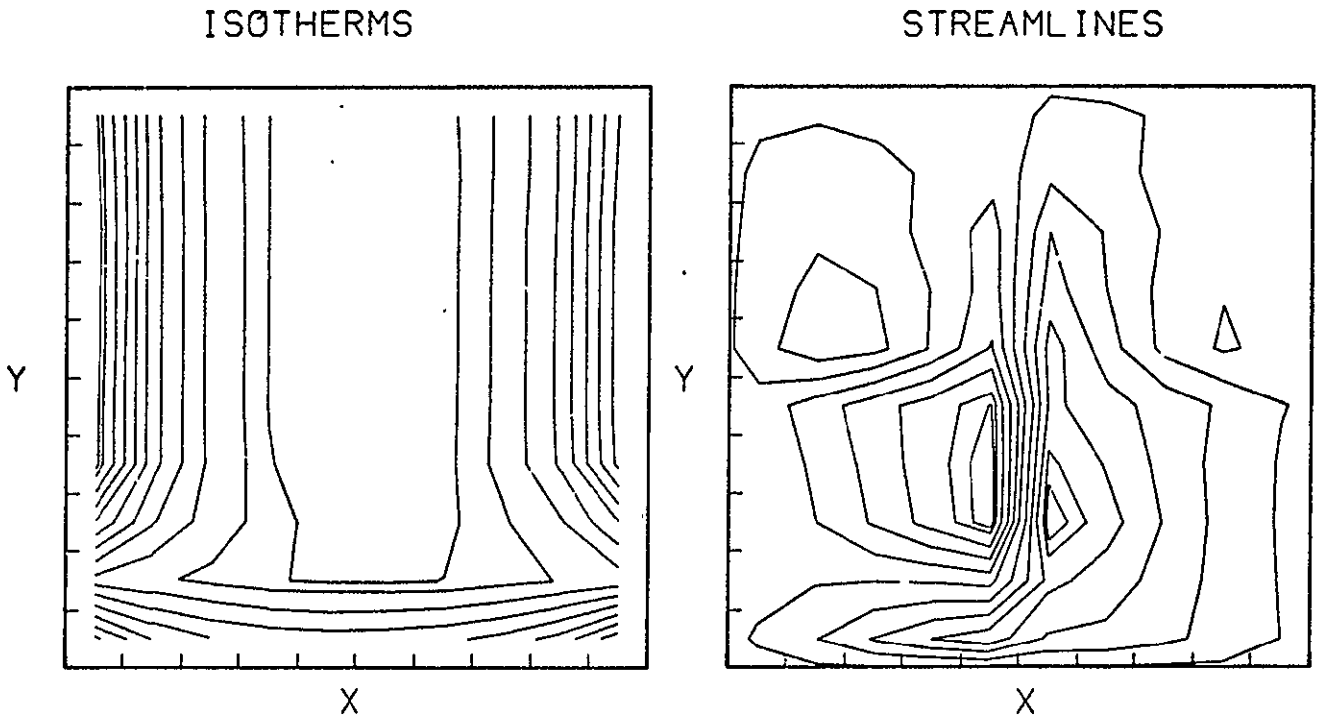

SPAR 74/21/3R FLIGHT TEST

Fig. 16 .- Continued

TIME = 40.0 (70 sec Flight Time)

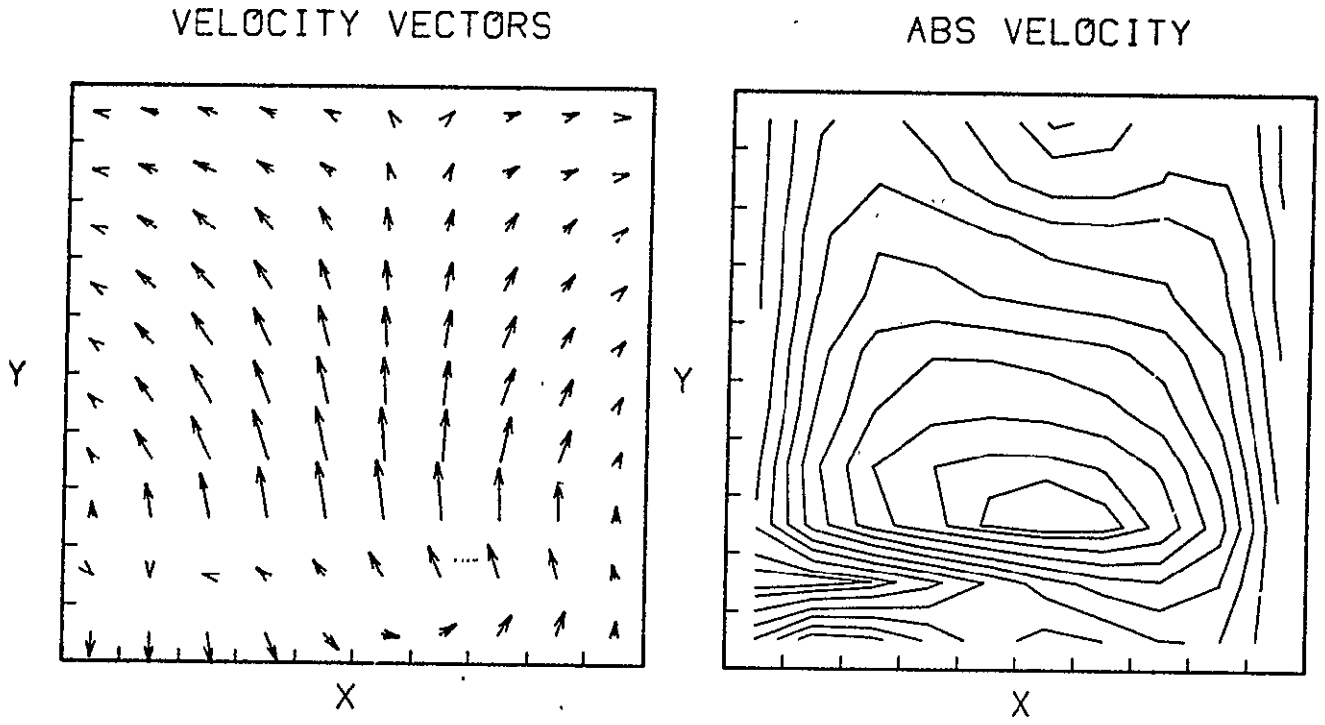

SPAR 74/21/3R FLIGHT TEST

Fig. 16 - Continued

TIME = 60.0 (90 sec Flight Time)

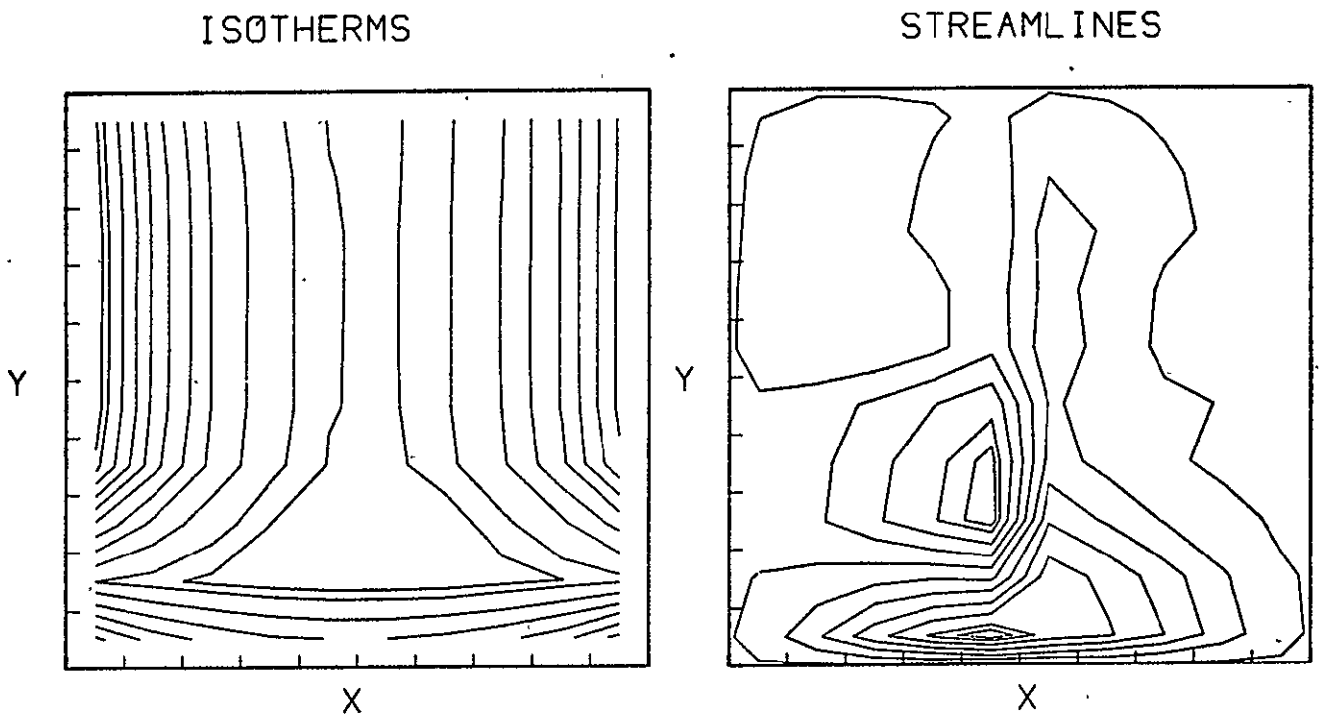

SPAR 74/21/3R FLIGHT TEST

Fig. 16 - Continued

TIME = 60.0 (90 sec Flight Time)

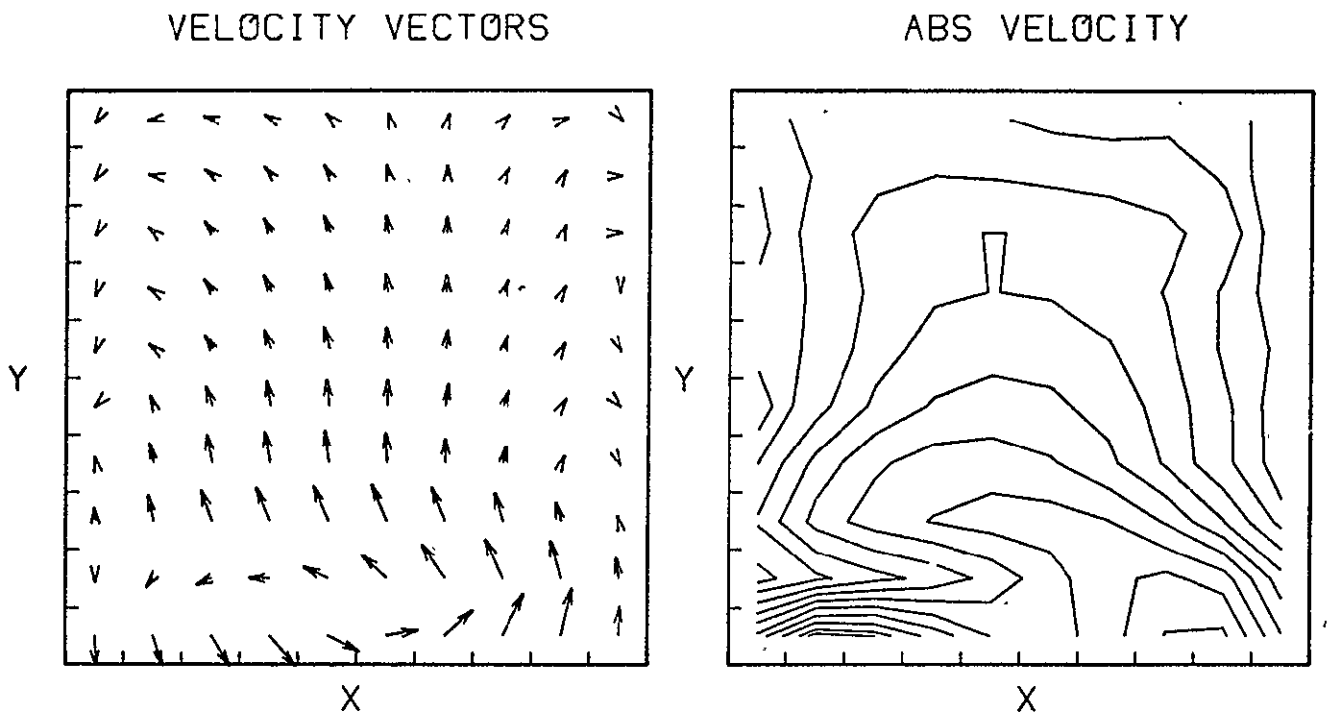

SPAR 74/21/3R FLIGHT TEST

Fig. 16 - Continued

TIME = 80.0 (110 sec Flight Time)

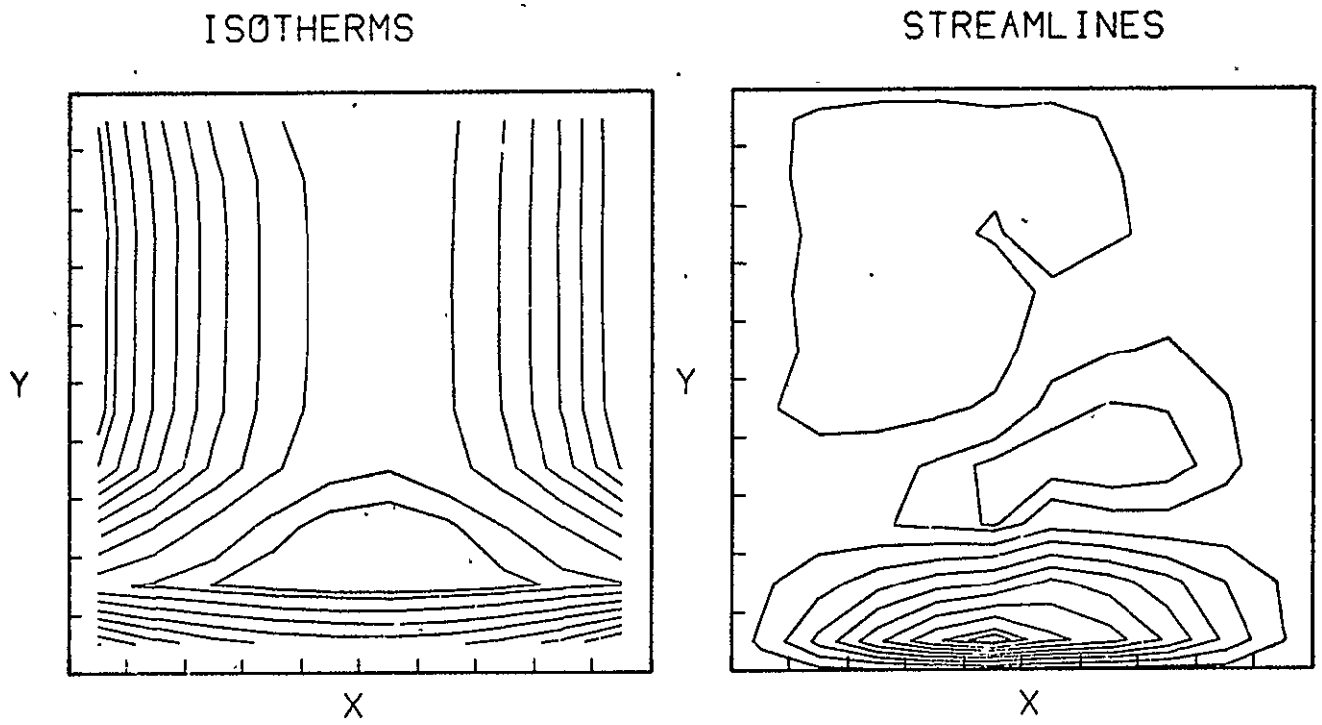

SPAR 74/21/3R FLIGHT TEST

Fig. 16 - Continued

TIME = 80.0 (110 sec Flight Time)

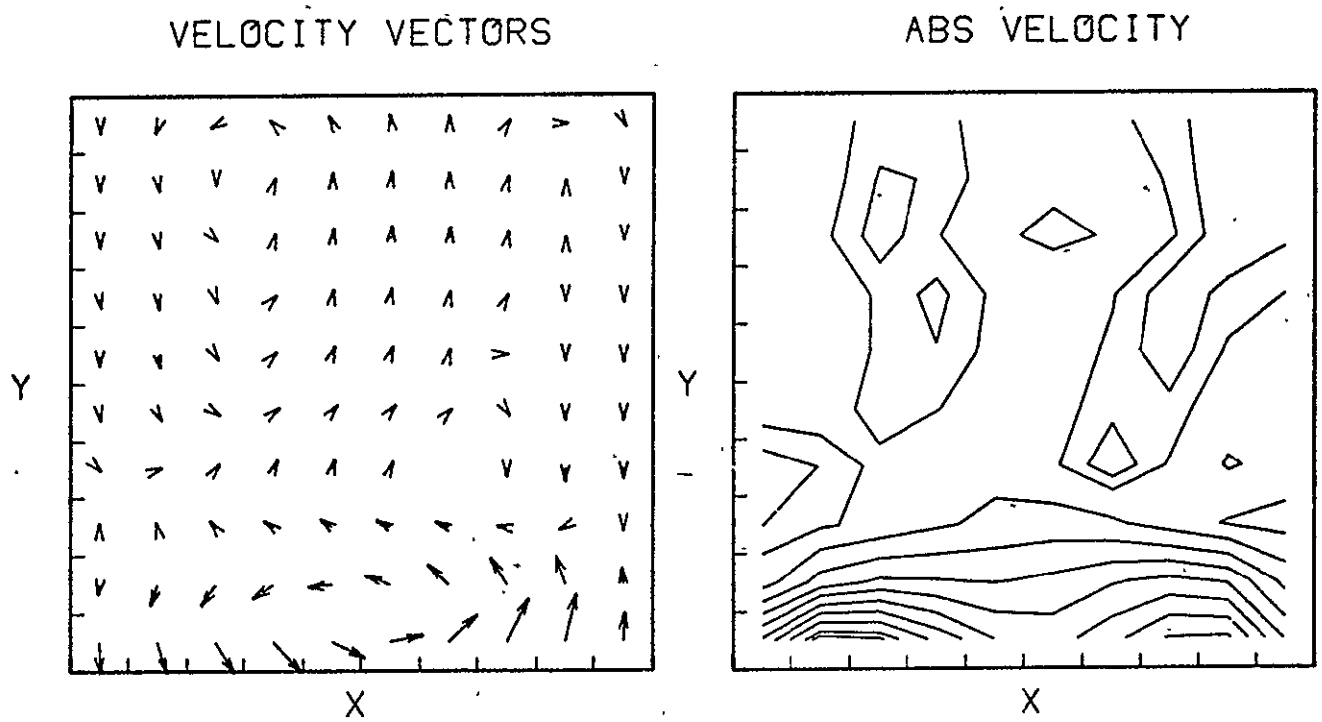

SPAR 74/21/3R FLIGHT TEST

Fig. 16 - Continued

TIME = 100.0 (130 sec Flight Time)

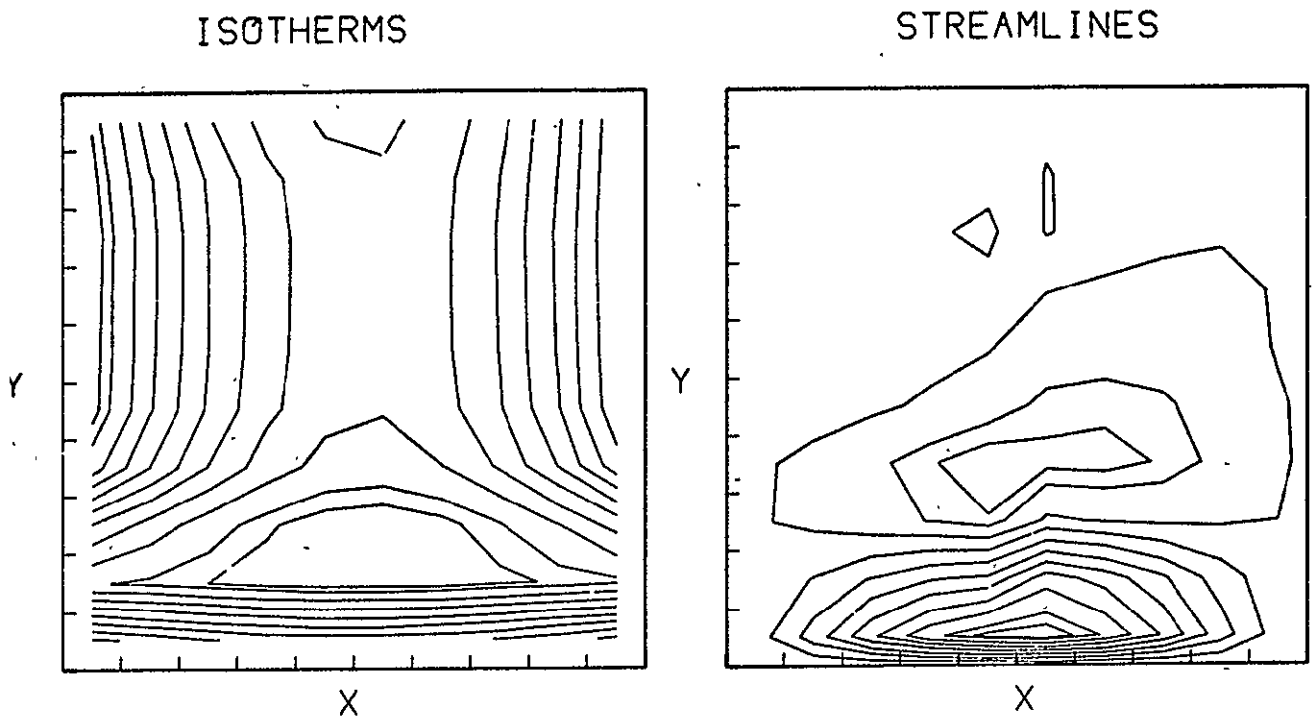

SPAR 74/21/3R FLIGHT TEST

Fig. 16 - Continued

TIME = 100.0 (130 sec Flight Time)

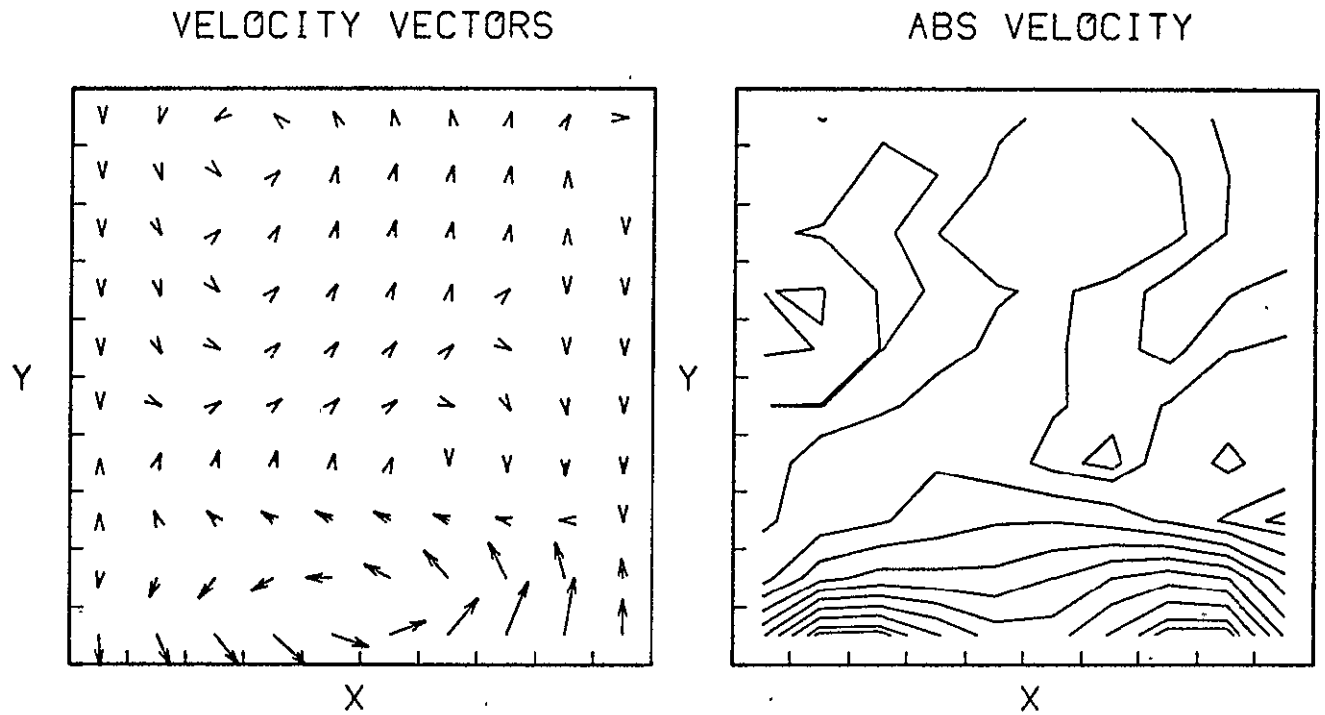

SPAR 74/21/3R FLIGHT TEST

Fig. 16 - Continued

TIME = 150.0 (180 sec Flight Time)

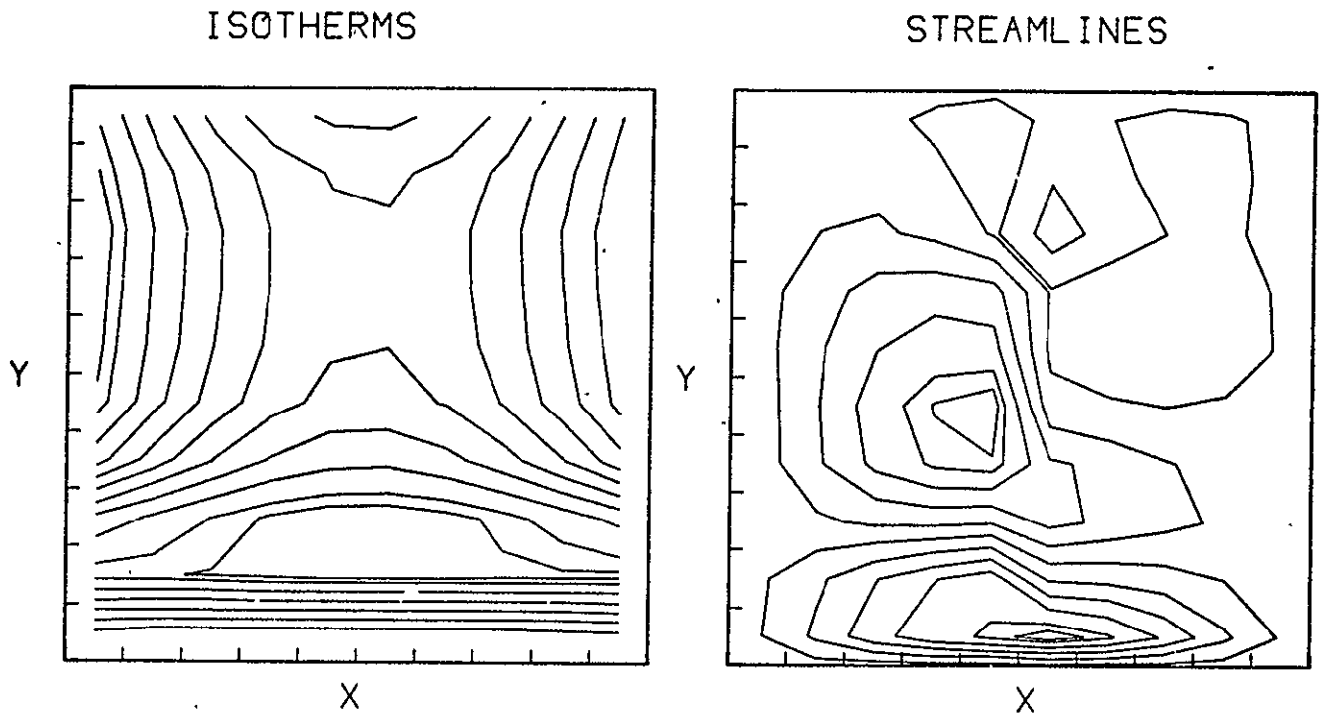

SPAR 74/21/3R FLIGHT TEST

Fig. 16 - Continued

TIME = 150.0 (180 sec Flight Time)

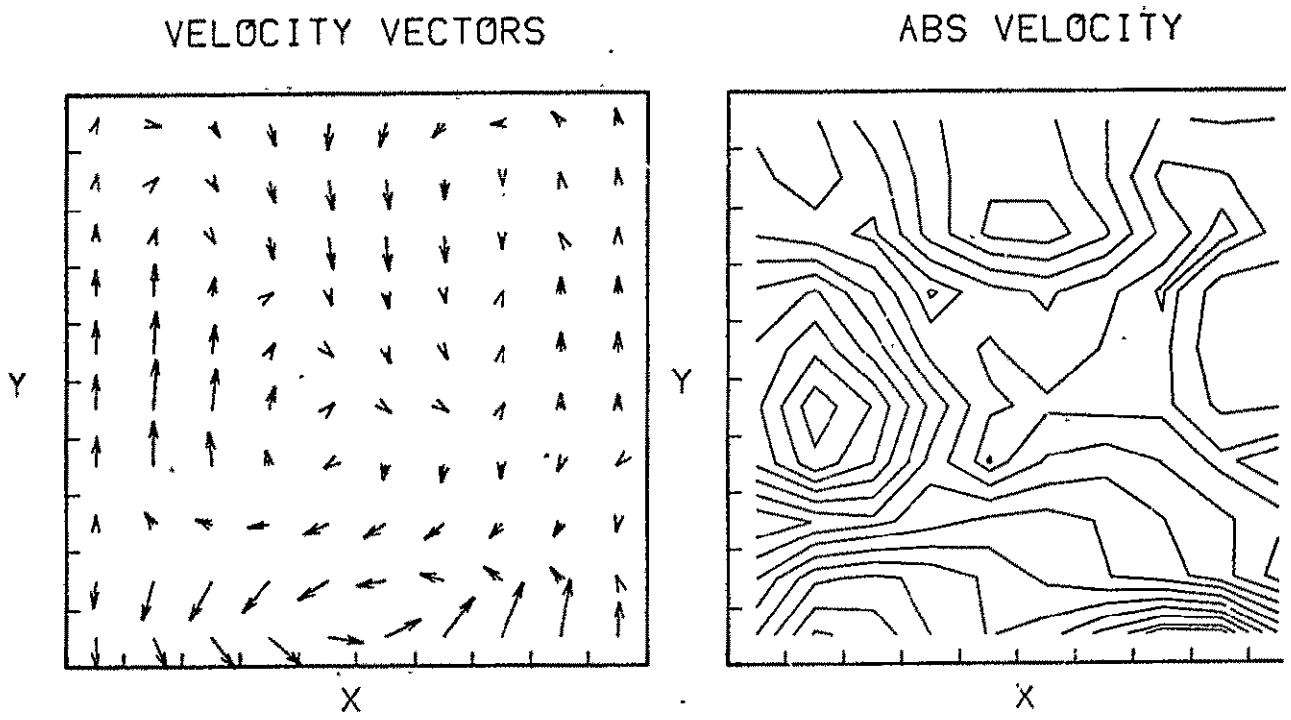

SPAR 74/21/3R FLIGHT TEST

Fig. 16 - Continued

TIME = 200.0 (230 sec Flight Time)

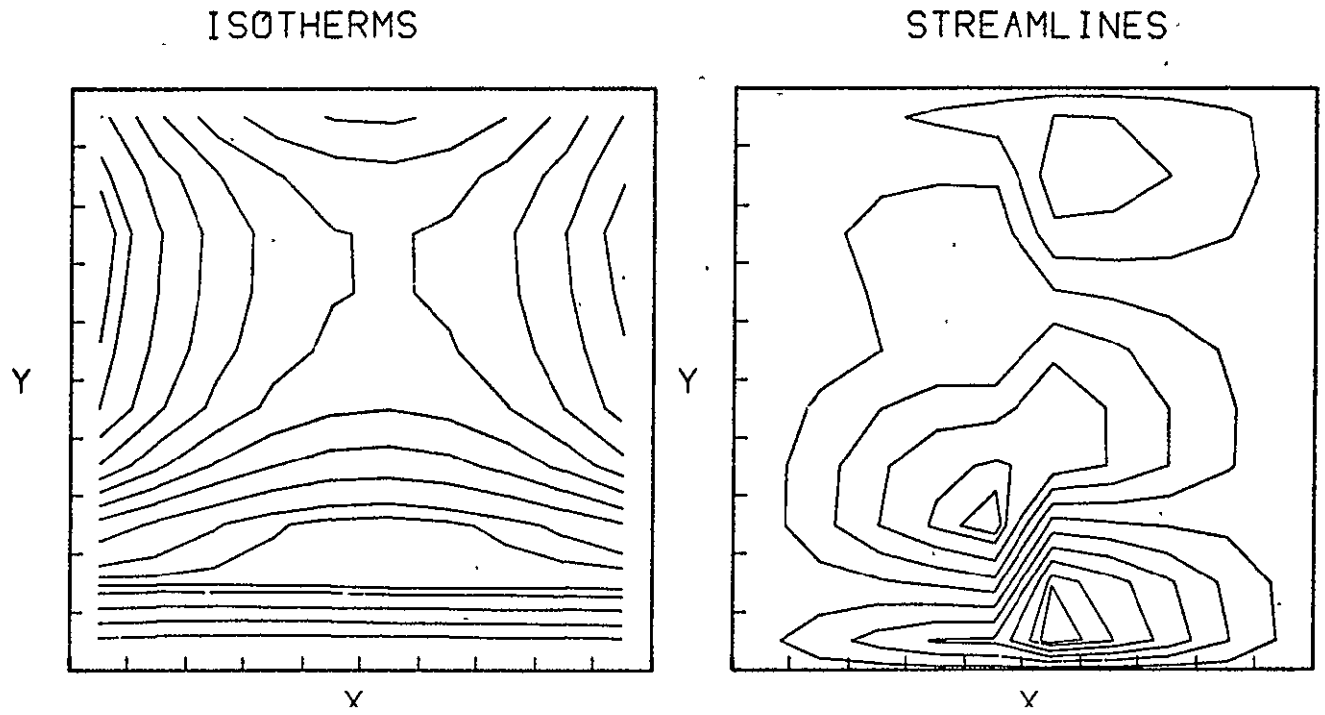

SPAR 74/21/3R FLIGHT TEST

Fig. 16 - Continued

TIME = 200.0 (230 sec Flight Time)

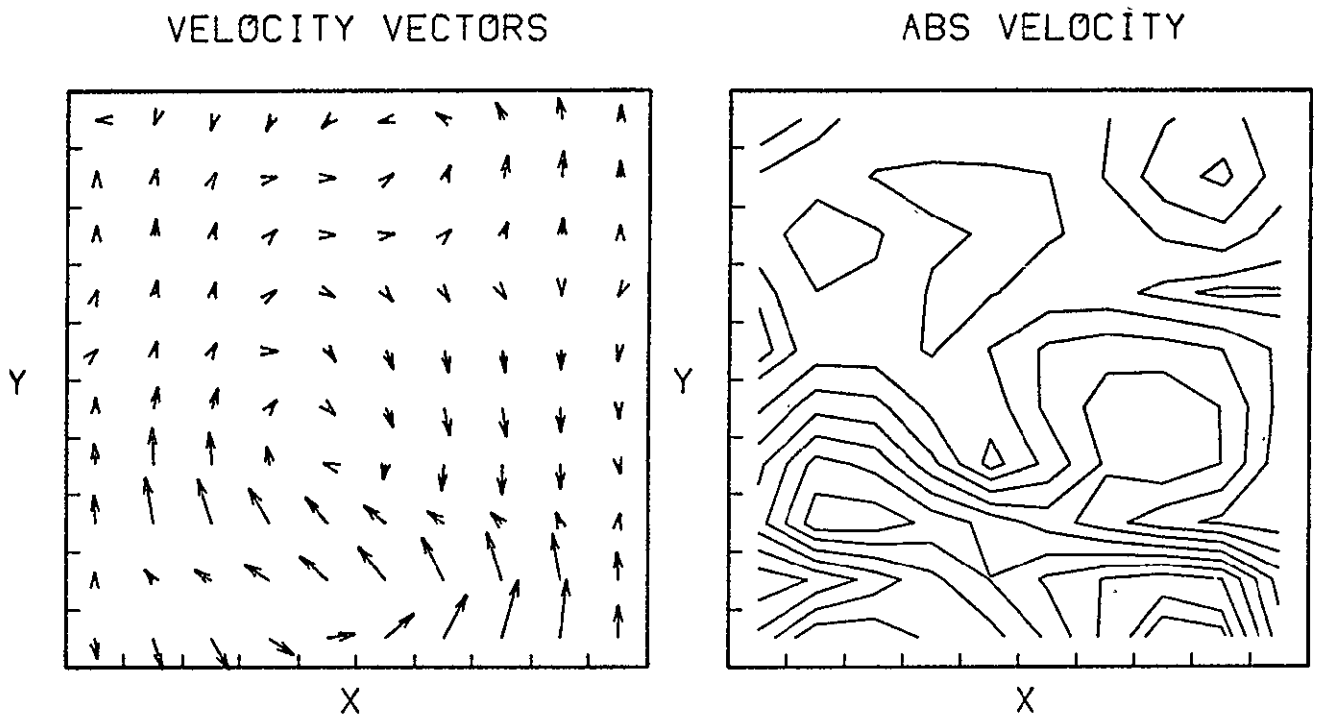

SPAR 74/21/3R FLIGHT TEST

Fig. 16 - Continued

TIME = 250.0 (280 sec Flight Time)

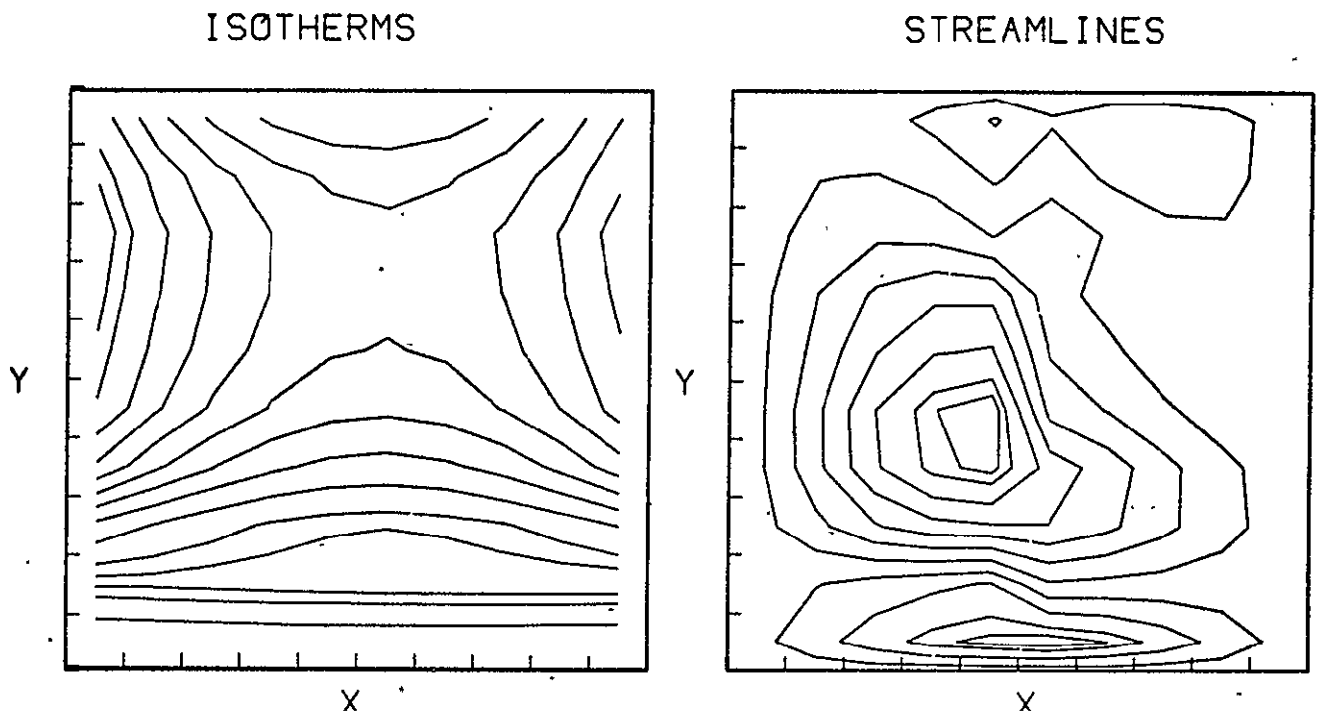

AR 74/21/3R FLIGHT TEST

Fig. 16 - Continued

TIME = 250.0 (280 sec Flight Time)

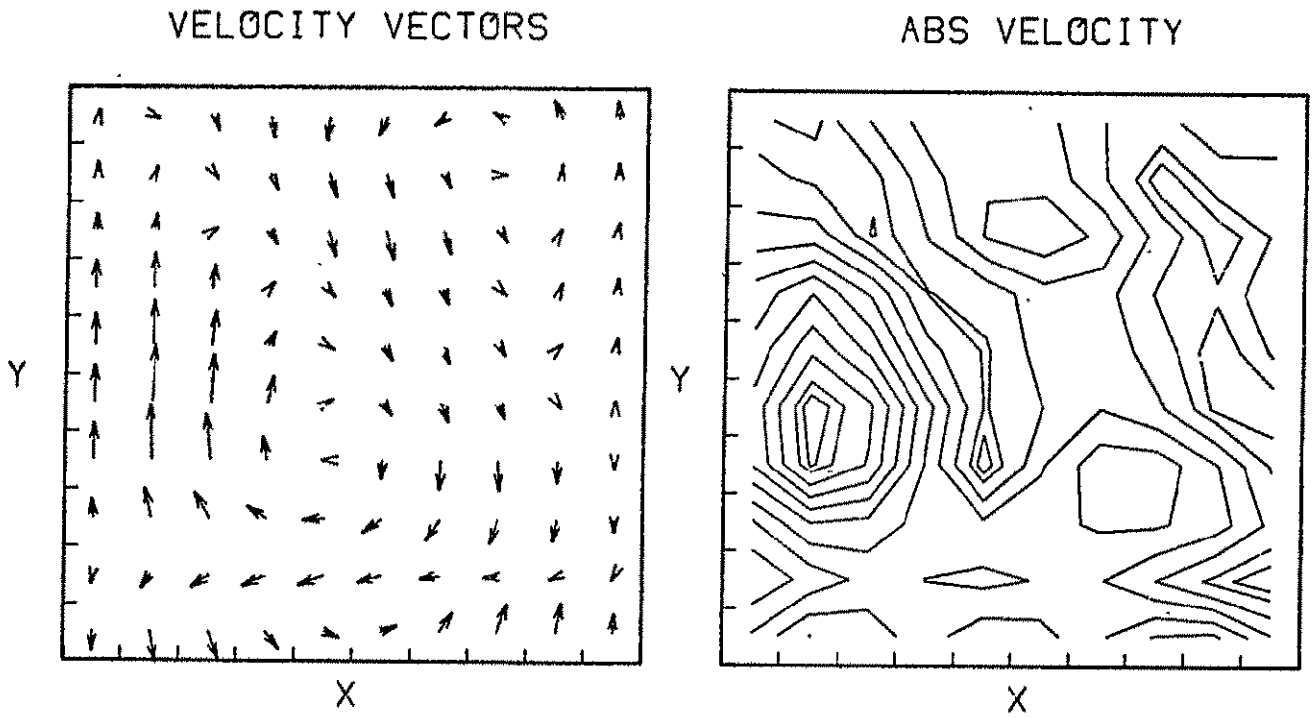

SPAR 74/21/3R FLIGHT TEST

Fig. 16 Continued

TIME = 300.0 (330 sec Flight Time)

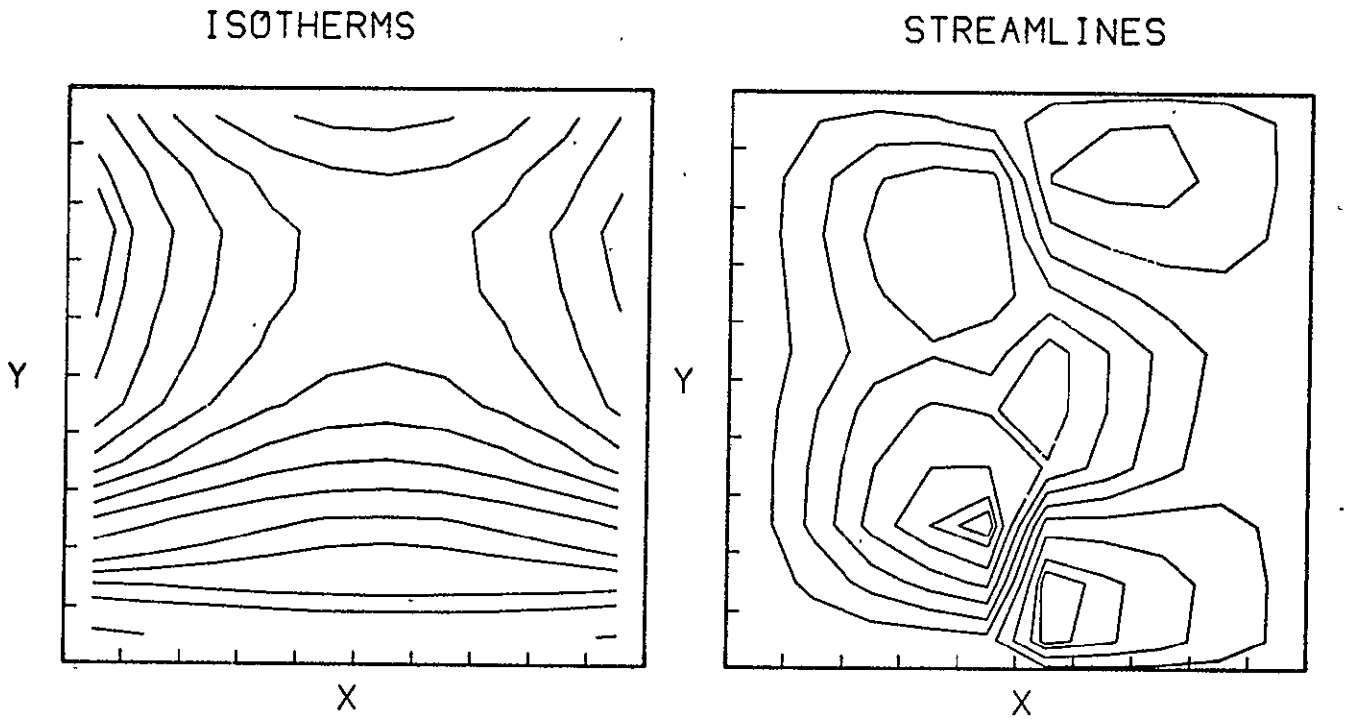

SPAR 74/21/3R FLIGHT TEST

Fig. 16 - Continued

TIME = 300.0 (330 sec Flight Time)

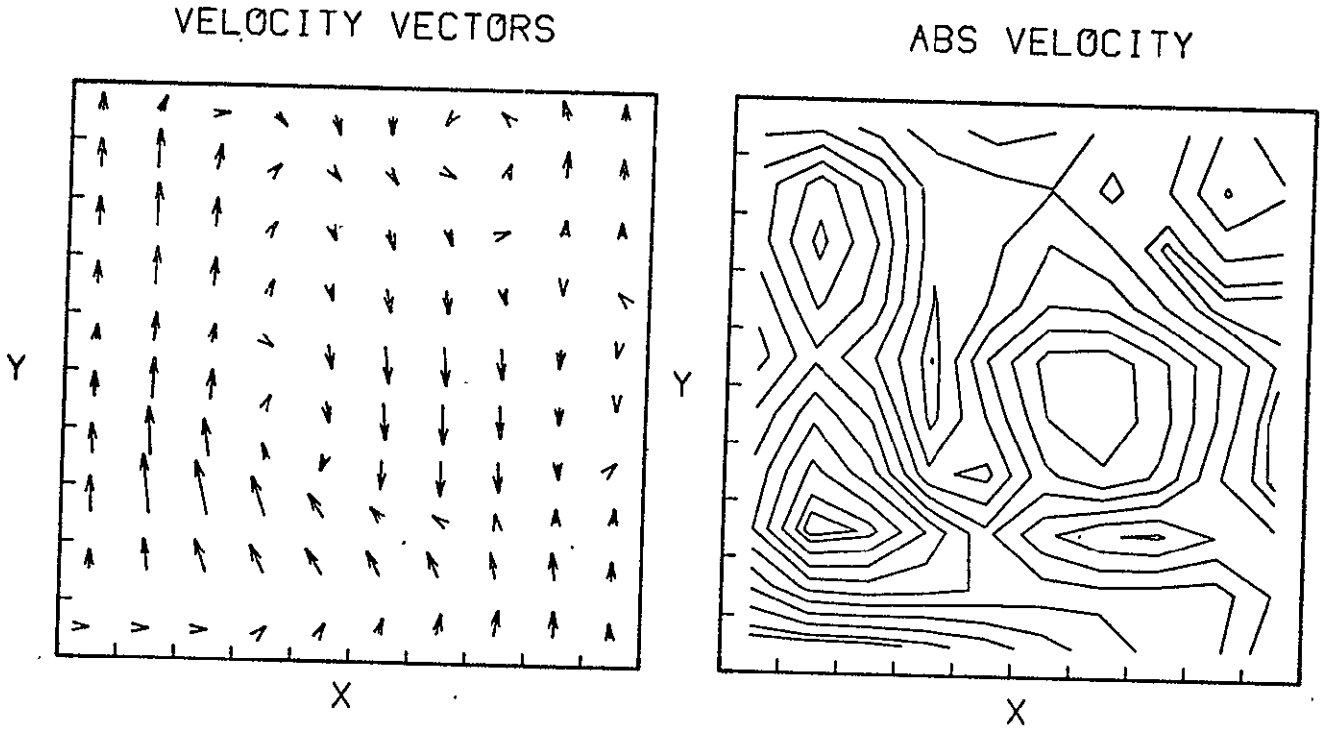

SPAR 74/21/3R FLIGHT TEST

Fig. 16 - Concluded

indicate that the T_7 surface started cooling somewhat prior to the T_4 and T_5 surfaces. This is reflected also in the isotherms shown in Fig. 16. As with the 74-21/2R experiment, the computed convective velocities were on the order of 10^{-5} cm/sec, indicating heat transfer essentially by pure conduction.

The centerline temperature distribution is shown in Fig. 17 at various flight times. Referring back to Fig. 15, the T_7 temperature measurement on the bottom surface reversed its decline after about 110 sec flight time and began to increase. This is reflected also in the computed temperatures near the surface shown in Fig. 17. The surface temperature gradient is seen to be about 30 C/cm, corresponding to a surface heat flux of -.036 cal/cm^2 sec The longitudinal component of gravity is away from the cooled surface with a magnitude of around 2×10^{-5} g_E (.02 cm/sec^2). Using Eq. (8), the Rayleigh number is

$$Ra_T = 4.5 \times 10^{-4} t^2 \tag{10}$$

where t is in sec. As previously found in the 74-21/2R flight test, the Rayleigh numbers are seen to be very low over the low gravity flight period, and, therefore, convective flow is not likely to be initiated by the density gradients at the cooled end. Lateral temperature distributions for various flight times are shown in Fig. 18 for a cross-section 3 cm from the end TED. This cross-section is about midway through the two side TED's. Up to about 160 sec, the surface temperature gradients are about 20 C/sec, indicating surface heat fluxes of about -.024 cal/cm^2 sec. For side cooling, the appropriate parameter for convective flow is the Grashof number:

$$Gr = \frac{g \beta_T \Delta T \delta^3}{\nu^2} \tag{11}$$

where, in this case, ΔT is the temperature difference from the center to an outside surface, and δ is one-half the width of the container. From Fig. 18, ΔT is about 7C, and δ is 0.5 cm. For $g = 2 \times 10^{-5}$ g_E (.02 cm/sec^2), the

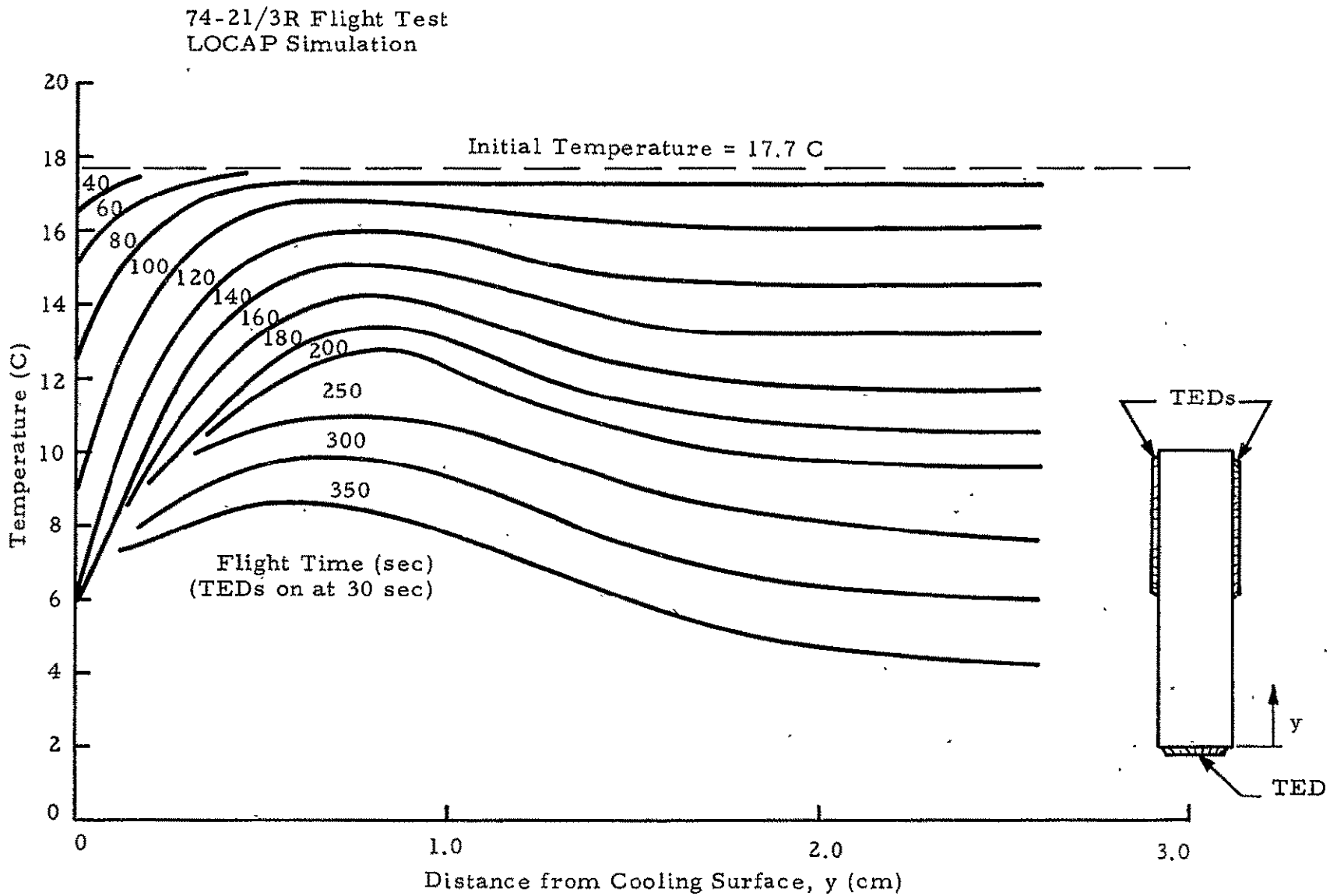

Fig. 17 - Centerline Temperature Distribution for 74-21/3R Flight Test for Various Flight Times

LOCKHEED - HUNTSVILLE RESEARCH & ENGINEERING CENTER

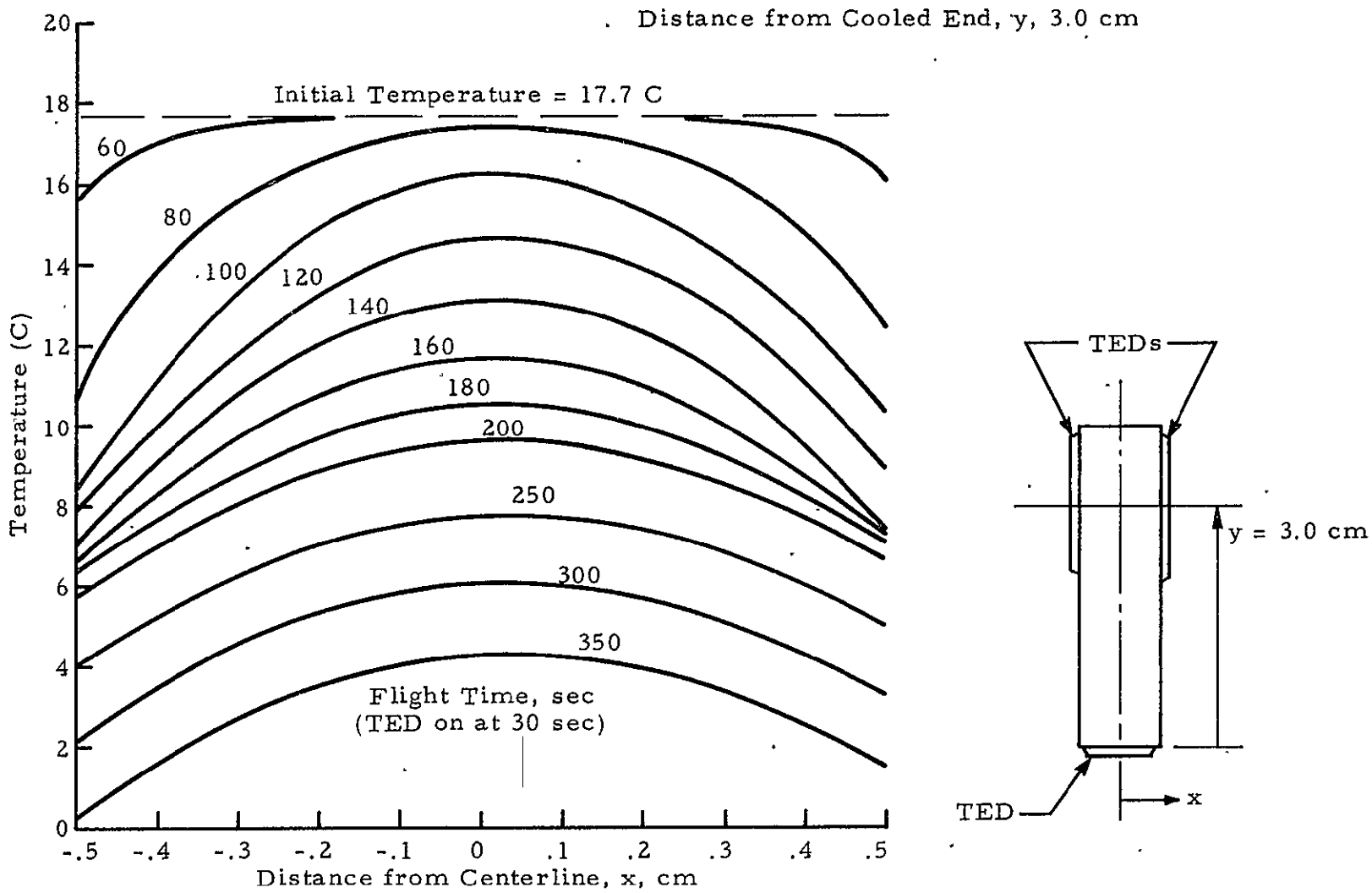

Fig. 18 - Lateral Temperature Distributions for 74-21/3R Flight Test for Various Flight Times

Grashof number is .009. From Ref. 7, the maximum velocity in the boundary layer for free convection on a vertical plate is given by:

$$U_{max} = \frac{.766\ \nu}{\delta} \left(.952 + \frac{\nu}{\alpha}\right)^{1/2} Gr^{1/2} \left(\frac{x}{\delta}\right)^{1/2} \qquad (12)$$

Assuming x equal to 2 cm, (the cooled distance on the side wall) the maximum velocity would be about .0026 cm/sec, compared to velocities on the order of 10^{-5} cm/sec calculated by the LOCAP program. Apparently, Eq. (12) over-estimates the convective velocities by up to two orders of magnitude. In either case, the thermal convective velocities for the flight test are very small.

4.3 RESULTS FOR 74-21/2R, GROUND TEST

The measured temperatures at the T_1, T_2 and T_3 locations for the 74-21/2R ground test are shown in Fig. 19 compared with the thermal analyzer simulations. Since the thermal analyzer program treats only pure conduction, these results are useful only as a first step to obtaining convective flow estimates. In reality, convective flows will be set up in the liquid under the one-g gravity conditions, so that heat transfer in the liquid will be increased.

The LOCAP program was found to be inappropriate for the ground test analyses because the one-g gravity level dictates a maximum time-step of only 10^{-4} sec, requiring exceedingly long run times to analyze a full test run. We analyzed the ground test convective flows by estimating expected velocities based on the Rayleigh and Grashof numbers. The 74-21/2R ground test was performed with the long container dimension in the vertical position with the cooling surface on bottom. Cooling from the bottom produces a hydrostatically stable configuration, except where the container side walls cool more rapidly than the adjacent liquid. This is the case in the 74-21/2R ground test. Lateral temperature distributions for various times are shown in Fig. 20 for a cross-section 0.55 cm from the bottom interior surface. This is the location of the first thermal analyzer program node point away from the bottom surface and

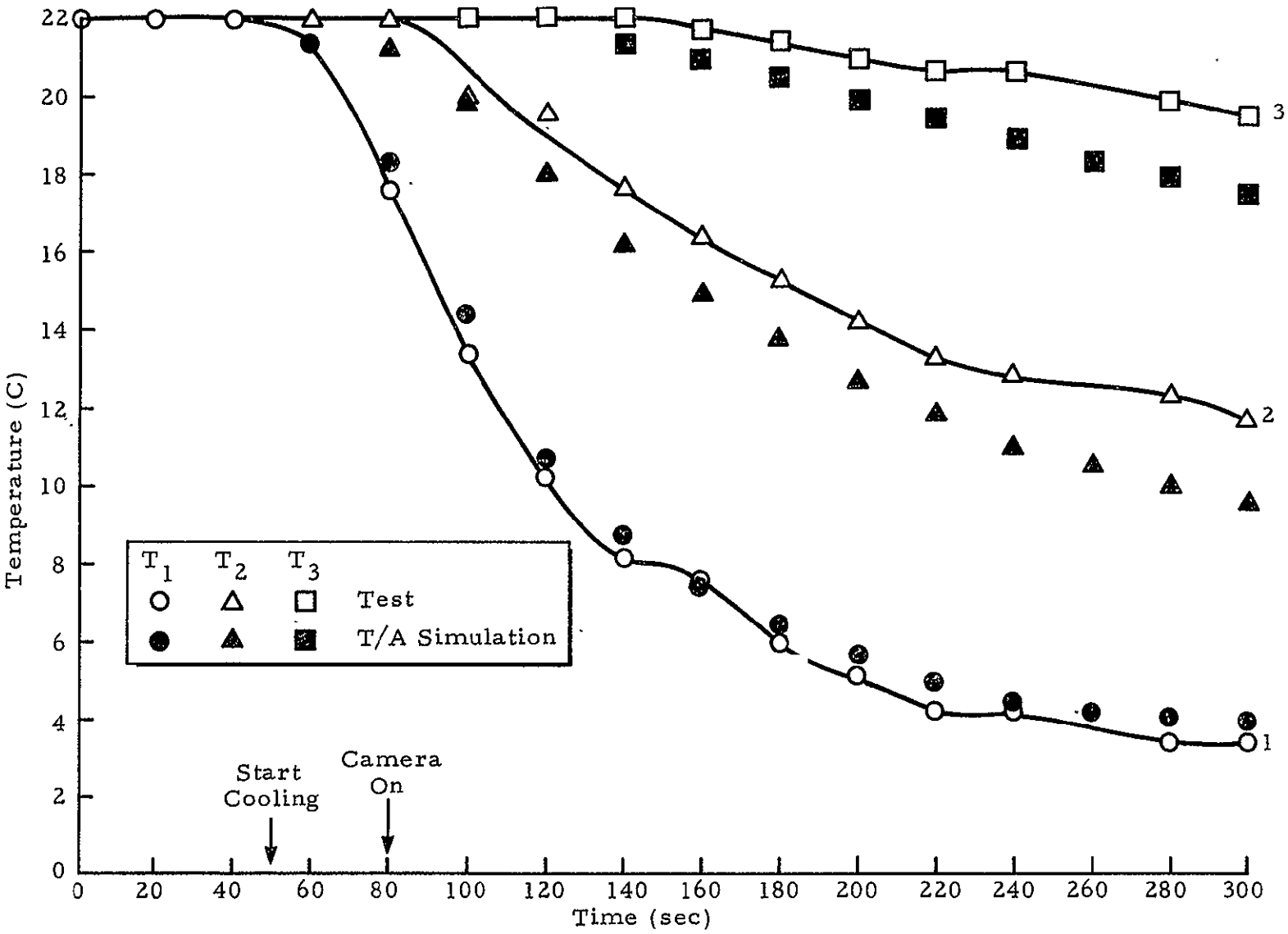

Fig. 19 - Measured Temperatures on 74-21/2R Ground Test Compared to Thermal Analyzer Simulation

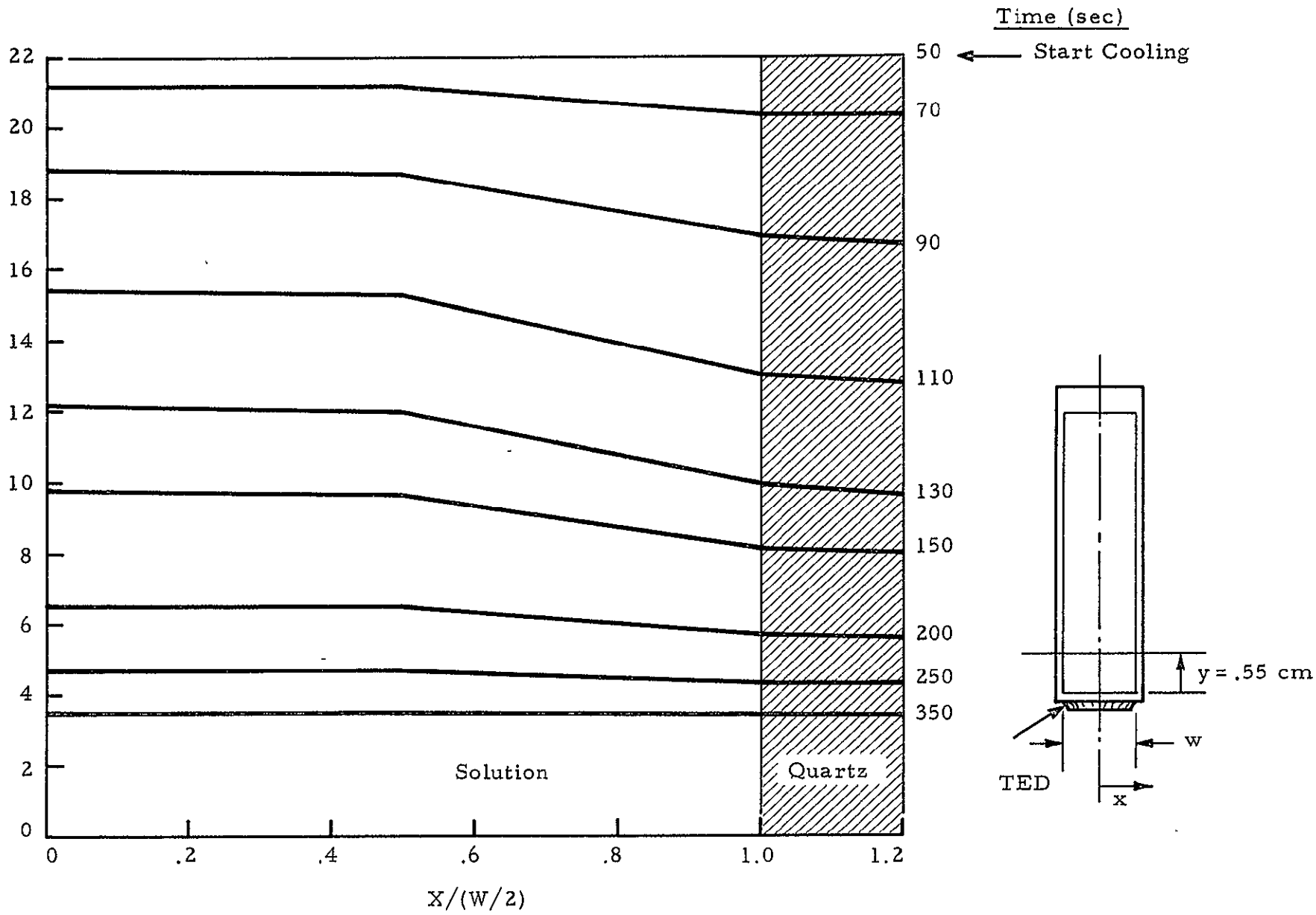

Fig. 20 - Lateral Temperature Distributions for 74-21/2R Ground Test for Various Test Times

The point indicating the greatest temperature difference between the container wall and adjacent liquid. The greatest temperature difference occurs at about 60 sec after initiation of cooling and is about 2 C over a distance of about 0.25 cm. From Eq. (11), this corresponds to a Grashof number of 104 and, from Eq. (12), a maximum velocity of 0.15 cm/sec. The cooling length x was assumed to be 0.5 cm. Thus, even in the supposedly stable configuration of cooling from the bottom, there is considerable convective motion.

4.4 RESULTS FOR 74-21/3R, GROUND TEST

The measured temperatures at the T_4, T_5, T_6 and T_7 locations on 74-21/3R during ground test are shown in Fig. 21 compared with the thermal analyzer simulation. Note that, as, in the flight test T_4, T_5 and T_7 measurements show good agreement with the simulations, while the T_6 measurement does not. Again, no definite explanation is available. The ground test was conducted with the long container dimension in the vertical position and with the end TED on bottom. The bottom cooling should induce little or no convective motion compared to the two sides. Lateral temperature distributions for various times are shown in Fig. 22 for a cross-section 3.2 cm from the bottom interior surface. This cross-section is about midway through the two side TEDs. Maximum temperature differences of about 6 C are noted over a distance of 0.5 cm. This corresponds to a Grashof number of 2500 (Eq. (11), and a resulting maximum velocity of about 0.5 cm/sec (Eq. (12)). Based on a characteristic dimension of 0.5 cm, this corresponds to a Reynolds number of 27, well within the range of laminar flow.

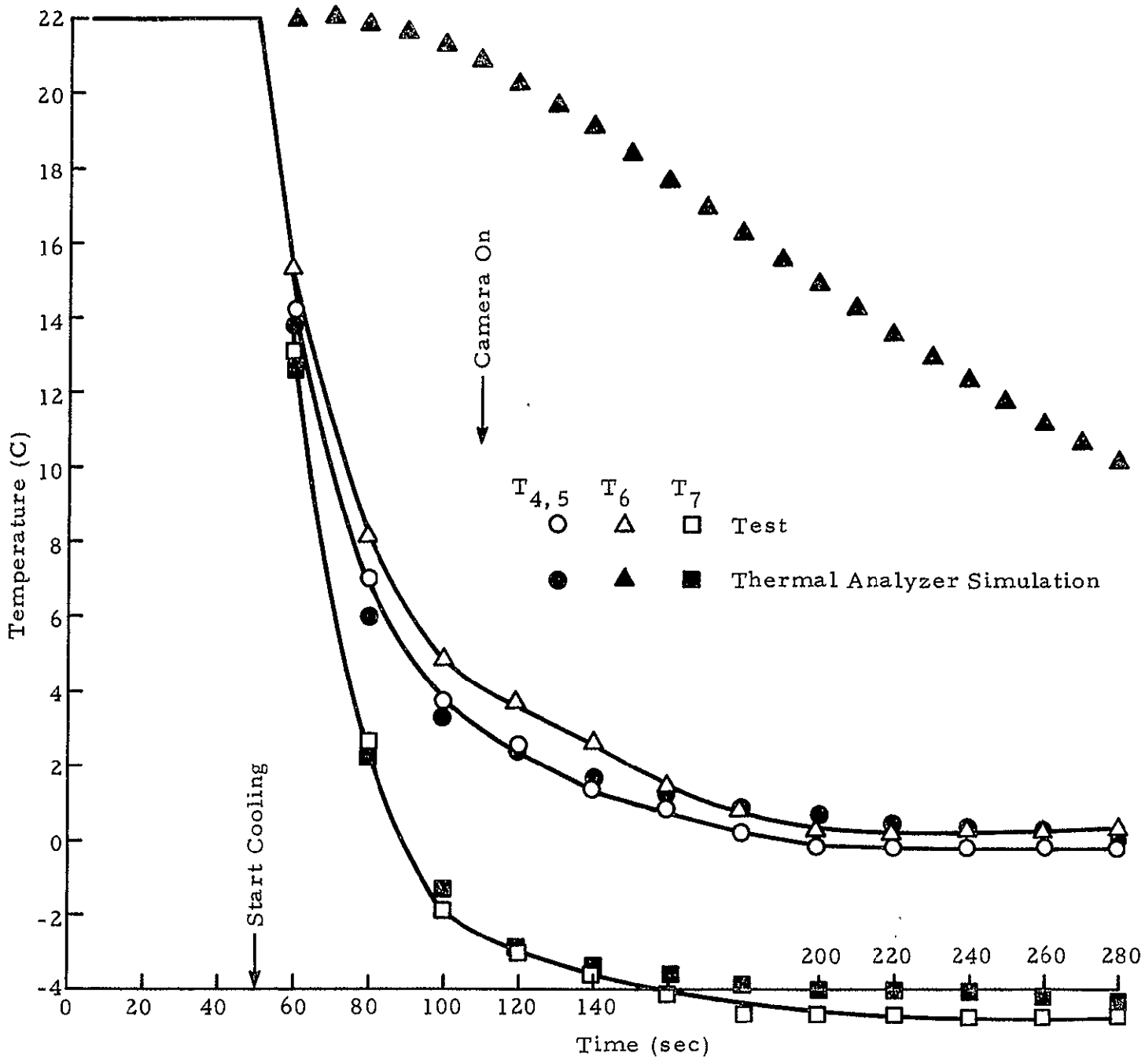

Fig. 21 - Measured Temperatures on 74-21/3R Ground Test Compared to Thermal Analyzer Simulation

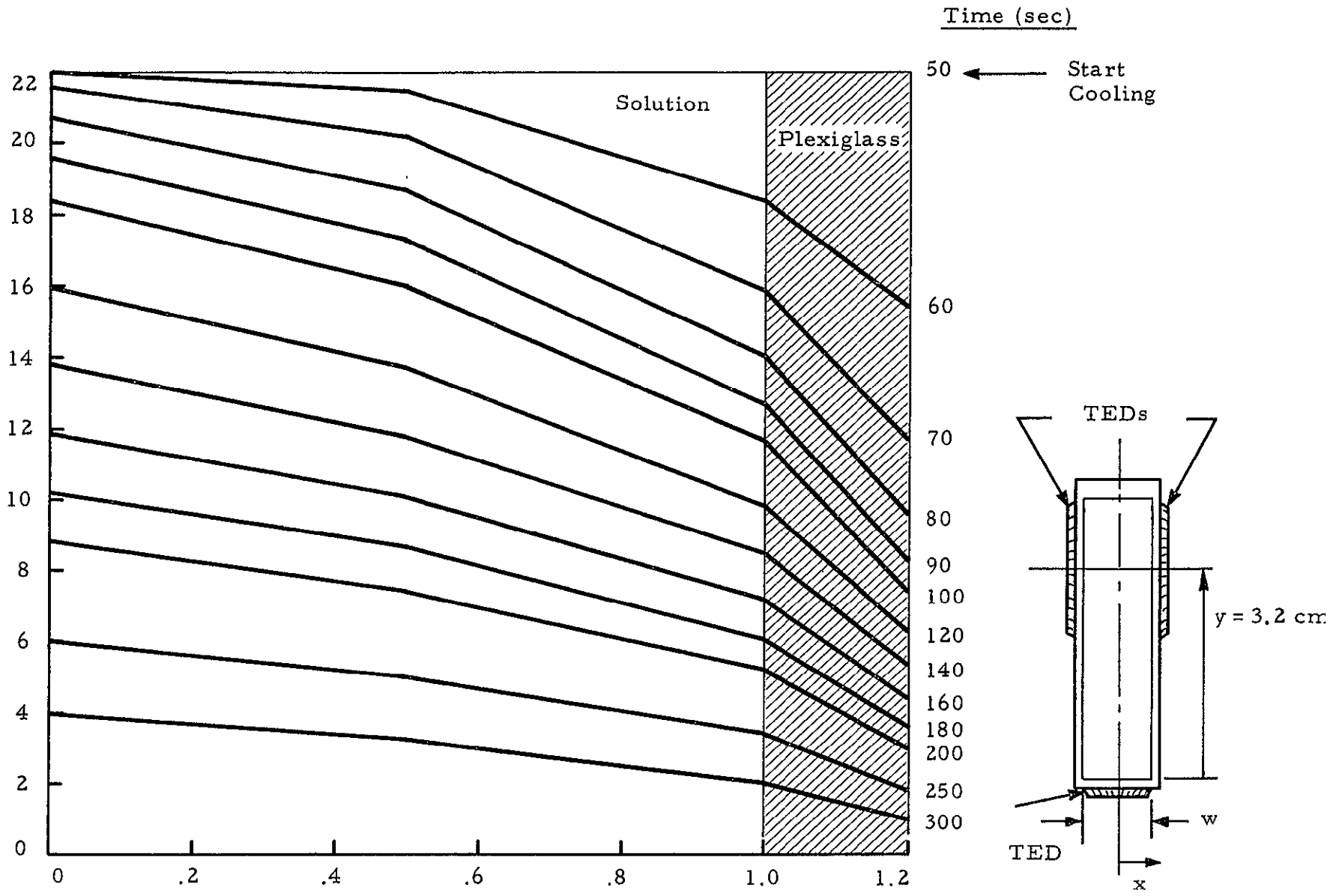

Fig. 22 - Lateral Temperature Distributions for 74-21/3R Ground Test for Various Test Times

5. SOLUTAL CONVECTION ANALYSIS

In attempting to simulate chemical diffusion effects using the LOCAP program, we found that the extremely low chemical diffusivity limited significant diffusion effects to a very thin layer adjacent to the solidifying interface. Thus, the LOCAP program would require an extremely fine grid to adequately simulate diffusion within this thin layer. For this reason, we elected to investigate the solutal effects in the thin layer using closed form, rather than numerical, analytical methods.

Mass flow with diffusion of a particular species in a moving fluid is described by

$$\vec{q} = C\,\vec{v}_\ell - D \text{ grad } C \tag{13}$$

where $\vec{q}$ is the mass flux of the particular species, C is concentration, $\vec{v}_e$ is fluid velocity and D is chemical diffusivity. At the interface, the mass flux q_o is:

$$q_o = \rho_s\, v_s \tag{14}$$

where ρ_s is the density of the crystal and v_s is crystal growth rate. From photographs taken during flight test, the crystal was observed to grow at an overall rate of about 1.28×10^{-2} cm/sec. Based on a density of 1.527 g/cm^3 for the $NH_4C\ell$ crystal, this corresponds to a mass flux at the interface of .0195 g/cm^2 sec. Neglecting fluid motion, Ref. 5 provides a solution to the diffusion equation for a constant flux at the interface:

$$C\,(x,t) = C_o - 2\,\frac{q_o\sqrt{Dt}}{D}\,\text{ierfc}\left(x/2\sqrt{Dt}\right) \tag{15}$$

where x is distance from the interface, t is time from the initiation of solidification and C_o is the initial concentration. The behavior of Eq. (15) is such that the concentration C (o, t) at the interface will decrease down to zero, and beyond that time Eq. (15) is no longer applicable. At the interface (x = 0), Eq. (15) becomes

$$C(o,t) = C_o - \frac{2\,q_o}{D}\sqrt{\frac{Dt}{\pi}} \tag{16}$$

and the time t_o required for the concentration to reach zero is

$$t_o = \pi D \left(\frac{C_o}{2\,q_o}\right)^2 \tag{17}$$

For an initial concentration C_o of 0.302 g/cm^3 (28 percent mass fraction), chemical diffusivity D of 1.8×10^{-5} cm^2/sec and mass flux q_o of .0195 g/cm^2 sec, t_o is .003 sec. Thus, the concentration at the interface drops down to zero almost immediately. Thereafter, the concentration is given by

$$C(x,t) = C_o \operatorname{erf}\left(x/2\sqrt{Dt}\right) \tag{18}$$

The diffusion distance δ from the interface is indicated from Eq. (18) by

$$\delta \sim 2\sqrt{Dt} \tag{19}$$

Thus, the diffusion distance is only 0.08 cm after 100 sec and 0.14 cm after 300 sec.

The solutal Rayleigh number Ra_s is defined as:

$$Ra_s = \frac{g\,\beta_s\,\Delta C\,\delta^3}{\nu D} \tag{20}$$

where β_s is the solute expansion coefficient and ΔC is the concentration difference over the distance δ.

During the 74-21/2R flight test, the gravity vector is directed away from the solidification interface. For the ammonium chloride solution, the solutal expansion coefficient β_s is negative ($\beta_s = -0.281$ per unit mass fraction), and the decrease in concentration near the interface results in a decreased density. This is equivalent to heating from above and is thus a hydrostatically stable configuration. Even if the gravity were directed toward the solidifying interface, assuming $g = 2 \times 10^{-5}\ g_E$ (.02 cm/sec^2) ΔC = 0.28 mass fraction and $\delta = 0.14$ cm, the Rayleigh number would be only about 25, which is well within the stable range. For the ground test, however, gravity is directed toward the solidifying interface and, for sufficiently high Rayleigh numbers, convective motion may be induced. Assuming $\Delta C = 0.28$ mass fraction and $\delta = 0.14$ cm, the solutal Rayleigh number is 1.25×10^6, definitely unstable. A solutal Grashof number Gr_s can be defined as

$$Gr_s = Ra_s/Sc \tag{21}$$

where

$$Sc = \nu/D \tag{22}$$

The Schmidt number Sc for the ammonium chloride solution is 516. The solutal Grashof number for the 74-21/2R ground test, therefore, is about 2422. Using the solutal equivalent of Eq. (12), with x being the width of the bottom surface, 1 cm, the estimated convective velocity is about 0.3 cm/sec, about the same as the thermal convective velocity.

For the 74-21/3R flight experiment, solidification on the side walls can result in some solutal convection. The solutal Rayleigh and Grashof numbers for the 74-21/3R experiment should be about the same as for 74-21/2R. Again using Eq. (12), with x being the length of the cooled surface on the side walls, 2 cm, the convective velocity is 0.0018 cm/sec, which is about half that due to thermal convection from the cooling surfaces (Section 4.2). The solutal

convection is also confined to a much thinner layer than the thermal convection.

Using the same equations, the solutal convection velocities for the 74-21/3R ground test are estimated to be about 0.4 cm/sec, about the same as the estimated thermal convection velocity.

6. CONCLUSIONS

The thermal convective velocities during the 74-21/2R and 74-21/3R flight tests were calculated using the LOCAP program to be of the order of 10^{-5} cm/sec, essentially negligible. As a comparison, an estimate was made using well known convection formulas for convection from the cooled side walls on 74-21/3R. The result was about 3×10^{-3} cm/sec, about two orders of magnitude greater than the LOCAP results, but still very small.

The 74-21/2R and 74-21/3R ground tests were analyzed using the closed form convection formulas, since the LOCAP program required extremely small time steps and, hence, long computer run times to analyze a full test run. Thermal convection velocities of 0.1 to 0.5 cm/sec were calculated for the 74-21/2R and 74-21/3R ground tests, two to four orders of magnitude greater than for the flight tests.

Because of the very low chemical diffusivity of the ammonium chloride solution, solutal effects were found to be confined to a relatively thin layer, about 1 mm thick, near the solidifying surface. The LOCAP program was not used to analyze these cases, since an extremely fine grid would be required for accuracy. For the 74-21/2R flight test, solutal effects should produce no convective motion. For the 74-21/3R flight test, closed form convection equations were used to estimate solutal convection velocities on the order of 10^{-3} cm/sec, the same order of magnitude as thermal velocities calculated using the same methods. Since the LOCAP program calculated thermal convection velocities of the order of 10^{-5} cm/sec, it is considered likely that the flight test solutal convection velocity estimates are conservative on the high side. The estimated ground test solutal convection velocities were estimated to be about 0.3 to 0.4 cm/sec, in the same range as the estimated ground test thermal convection velocities.

REFERENCES

1. Benton, E.R., and A. Clark, Jr., "Spin-Up," Annual Review of Fluid Mechanics, Vol. 6, (M. Van Dyke, W.G. Vincenti and J.V. Wehausen, Eds.), Annual Reviews, Inc., Palo Alto, Calif., 1974.
2. McLeod, A.R., "The Unsteady Motion Produced in a Uniformly Rotating Cylinder of Water by a Sudden Change in the Angular Velocity of the Boundary," Phil. Mag., S. 6, Vol. 44, No. 259, July 1922.
3. Weidman, P.D., "On the Spin-Up and Spin-Down of a Rotating Fluid. Part 1 Extending the Wedemeyer Model," J. Fluid Mech., Vol. 77, Part 4, p. 685, 1976.
4. Weidman, P.D., "On the Spin-Up and Spin-Down of a Rotating Fluid. Part 2 Measurements and Stability," J. Fluid Mech., Vol. 77, Part 4, p. 709, 1976.
5. Carslaw, H.C., and J.C. Jaeger, Conduction of Heat in Solids, Oxford University Press, 1959.
6. Chansdrasekhar, S., Hydrodynamic and Hydromagnetic Stability, Oxford University Press, 1968.
7. Eckert, E.R.G., and R.M. Drake, Jr., Heat and Mass Transfer, McGraw-Hill, New York, 1959.